Published August 5, 2013

Macrophage-secreted cytokines drive pancreatic acinar-to-ductal metaplasia through NF-κB and MMPs

Geou-Yarh Liou,[1] Heike Döppler,[1] Brian Necela,[1] Murli Krishna,[2] Howard C. Crawford,[1] Massimo Raimondo,[3] and Peter Storz[1]

[1]Department of Cancer Biology, Mayo Clinic Comprehensive Cancer Center, [2]Department of Laboratory Medicine and Pathology, and [3]Division of Gastroenterology and Hepatology, Mayo Clinic, Jacksonville, FL 32224

In response to inflammation, pancreatic acinar cells can undergo acinar-to-ductal metaplasia (ADM), a reprogramming event that induces transdifferentiation to a ductlike phenotype and, in the context of additional oncogenic stimulation, contributes to development of pancreatic cancer. The signaling mechanisms underlying pancreatitis-inducing ADM are largely undefined. Our results provide evidence that macrophages infiltrating the pancreas drive this transdifferentiation process. We identify the macrophage-secreted inflammatory cytokines RANTES and tumor necrosis factor α (TNF) as mediators of such signaling. Both RANTES and TNF induce ADM through activation of nuclear factor κB and its target genes involved in regulating survival, proliferation, and degradation of extracellular matrix. In particular, we identify matrix metalloproteinases (MMPs) as targets that drive ADM and provide in vivo data suggesting that MMP inhibitors may be efficiently applied to block pancreatitis-induced ADM in therapy.

Introduction

Cells of the adult pancreas can undergo reprogramming events by which they convert between different epithelial phenotypes, and this transformation can contribute to pancreatic cancer (Esni et al., 2005; Morris et al., 2010b; Puri and Hebrok, 2010). The transdifferentiation of acinar cells to a ductlike phenotype (acinar-to-ductal metaplasia [ADM]) can be induced by activating K-ras mutations (Hingorani et al., 2003), epidermal growth factor receptors (Wagner et al., 1998; Means et al., 2005), or pancreatic inflammation (pancreatitis; Carrière et al., 2007; Strobel et al., 2007; Zhu et al., 2007), all of which have been implicated to contribute to development of pancreatic cancer (Cano et al., 2007; Guerra et al., 2007, 2011). The formation of ADM lesions is a reversible process (Cano et al., 2007; Puri and Hebrok, 2010; Collins et al., 2012). However, the resulting ductlike cells can also lead to formation of metaplastic duct lesions that are consistently found in pancreatitis (Song et al., 1999) or other precancerous lesions known as pancreatic intraepithelial neoplasia (PanIN; Hruban et al., 2001; Strobel et al., 2007). Eventually, PanIN can further progress to pancreatic ductal adenocarcinoma (PDAC) once cells acquire additional transforming mutations (Bardeesy and DePinho, 2002).

Transgenic and knockout animal models have shown the importance of TGF-α and activating mutations of K-ras as drivers of ADM and PanIN formation (Morris et al., 2010b). In experimental animal models, pancreatitis can be induced by the oligopeptide caerulein, which stimulates pancreatic secretion of digestive enzymes. In the presence of activating K-ras mutations, caerulein-induced pancreatic inflammation contributes to development of pancreatic adenocarcinoma (Guerra et al., 2007, 2011). The molecular signaling mechanisms that regulate ADM in response to pancreatitis are largely undefined. Pancreatitis, both in human patients and upon caerulein treatment in mice, elicits macrophage infiltration into the pancreas (Guerra et al., 2011). The contribution of macrophages to cancer is well known, but mechanistic insights of signaling events driving tumor initiation processes are unclear (Coussens and Werb, 2002).

Correspondence to Peter Storz: storz.peter@mayo.edu

Abbreviations used in this paper: ADM, acinar-to-ductal metaplasia; CK-19, cytokeratin-19; EGFR, EGF receptor; G-CSF, granulocyte colony-stimulating factor; H&E, hematoxylin and eosin; IHC, immunohistochemistry; JE, junctional epithelium; MMP, matrix metalloproteinase; NAB, neutralizing antibody; NF-κB, nuclear factor κB; PanIN, pancreatic intraepithelial neoplasia; PDAC, pancreatic ductal adenocarcinoma.

© 2013 Liou et al. This article is distributed under the terms of an Attribution–Noncommercial–Share Alike–No Mirror Sites license for the first six months after the publication date (see http://www.rupress.org/terms). After six months it is available under a Creative Commons License (Attribution–Noncommercial–Share Alike 3.0 Unported license, as described at http://creativecommons.org/licenses/by-nc-sa/3.0/).

Supplemental Material can be found at:
/content/suppl/2013/08/01/jcb.201301001.DC1.html
/content/suppl/2013/08/15/jcb.201301001.DC2.html

The Rockefeller University Press $30.00
J. Cell Biol. Vol. 202 No. 3 563–577
www.jcb.org/cgi/doi/10.1083/jcb.201301001

THE JOURNAL OF CELL BIOLOGY

Downloaded from on April 4, 2017

Published August 5, 2013

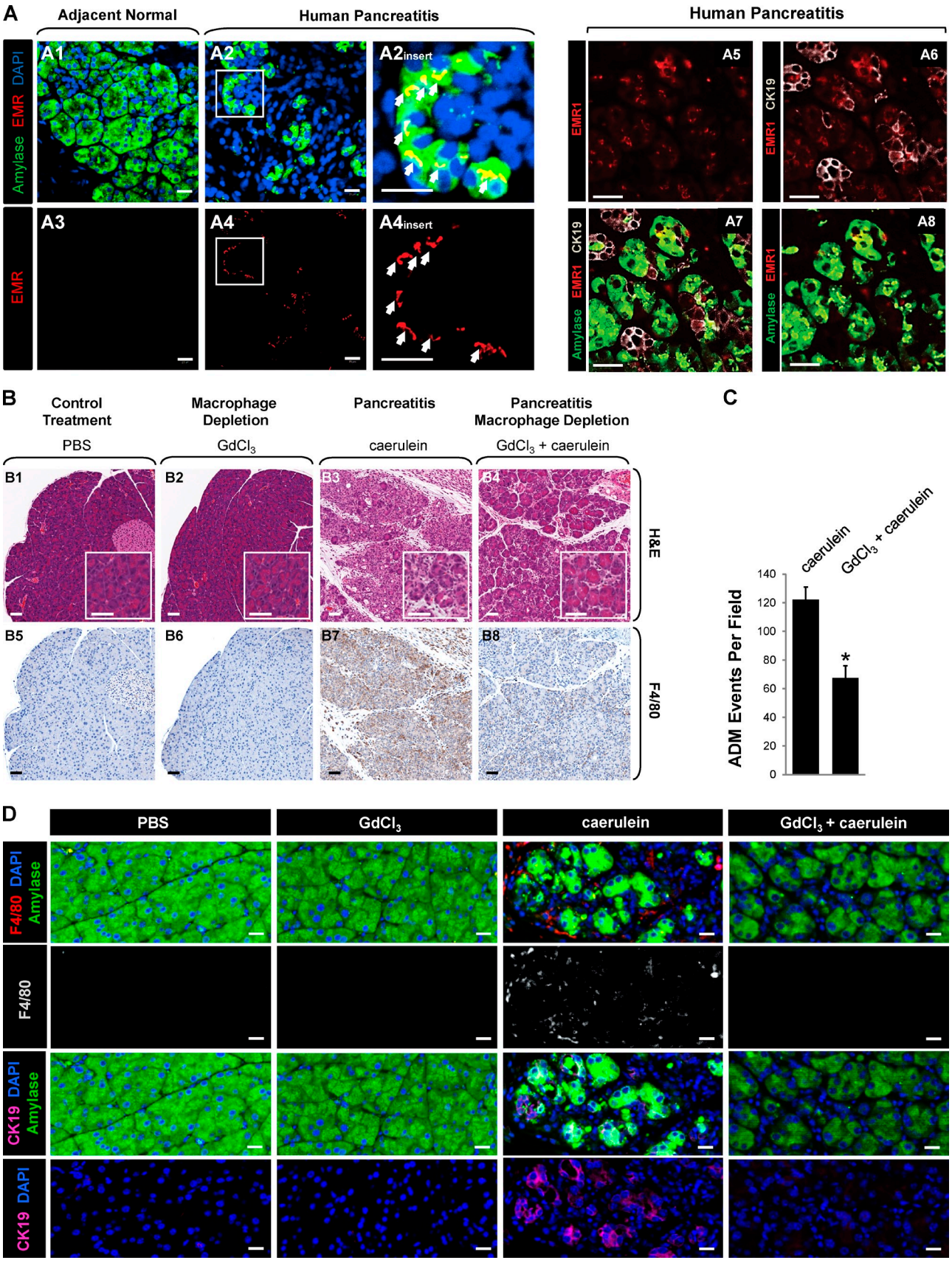

Figure 1. **Depletion of macrophages blocks pancreatic ADM.** (A) Samples of human pancreatitis or adjacent normal tissue were stained by immunofluorescence for macrophages (EMR1), amylase, CK-19 (gray in A6), and DAPI as indicated. Bars, 20 µm. (B) FVB mice were treated with control vehicle, $GdCl_3$, caerulein, or a combination, as indicated (detailed method in Materials and methods section). Pancreata were harvested and IHC stained with H&E or the

Downloaded from on April 4, 2017

Published August 5, 2013

This prompted our investigation of macrophage involvement in initiating ADM.

Here, we show that macrophage-secreted inflammatory cytokines are inducers of pancreatitis-initiated acinar cell reprogramming to a ductal progenitor phenotype. Because such ductlike cells can lead to PanIN lesions and PDAC, we provide evidence for a mechanism of how inflammation of the pancreas can induce a setup for tumor initiation, which eventually occurs when additional K-ras mutations are acquired (Guerra et al., 2007, 2011). We further establish the transcription factor nuclear factor κB (NF-κB) and its target genes as substantial drivers of acinar-to-ductal transdifferentiation. Because high NF-κB levels were observed in pancreatic cancer, but not in normal acinar tissue, our data also provide a mechanistic link between acinar cell reprogramming and pancreatic cancer. The identification of matrix metalloproteinases (MMPs) as one target group for NF-κB signaling that drive ADM suggests that MMP inhibitors may be efficiently applied to pancreatitis patients to block pancreatitis-induced ADM in therapy.

Results

Depletion of macrophages blocks pancreatic ADM

When comparing samples of human pancreatitis to normal pancreatic tissue, we found that in pancreatitis, macrophages attach to acinar cells in the pancreas that undergo ADM (Fig. 1 A). To investigate the role of macrophages in driving the ADM process, we next used an established mouse model in which the intraperitoneal injection of caerulein induces inflammation of the pancreas and acinar-to-ductal transdifferentiation (Morris et al., 2010a). Macrophage depletion by administration of the macrophage toxin $GdCl_3$ (gadolinium chloride hexahydrate) partially blocked ADM mediated by induction of pancreatitis (Fig. 1, B and C). This suggested that macrophages may be directly involved in regulating the processes that can lead to acinar-to-ductal transdifferentiation. As expected, mice depleted of macrophages also show decreased expression of connective tissue mucins in the pancreas as indicated by Alcian blue staining (Fig. S1 A). Immunofluorescence analysis using amylase as a marker for acinar cells, CK-19 for ductlike cells, and F4/80 as a marker for macrophages showed normal pancreas morphology for PBS- and $GdCl_3$ control–treated mice (Fig. 1 D). Mice treated with caerulein showed abundance of macrophages at acini undergoing ADM correlating with a decrease in the acinar marker amylase and increased expression of CK-19. Treatment with $GdCl_3$ protected from caerulein-induced dedifferentiation of acinar cells and pancreatic reorganization, suggesting a role for macrophages in these processes. Moreover, we found that after depletion of macrophages, T cells (CD3 positive) and neutrophils (Ly6B.2 positive) were still present in the pancreas at levels similar to those detected in pancreata of animals treated with caerulein alone (Fig. S1 B). This suggests a specific role for macrophages as drivers of ADM and reorganization of the pancreas. We also determined whether ADM is inhibited when pancreatitis is induced before or simultaneously to macrophage depletion. When animals were treated with caerulein before $GdCl_3$, pancreatic inflammation and ADM were not reduced, whereas when animals were treated simultaneously, inflammation was slightly reduced, correlating with reduced occurrence of macrophages in the pancreas (Fig. S1 C). In both treatment procedures, caerulein-induced presence of other immune cells was unaffected by $GdCl_3$. This indicates that macrophages specifically contribute to pancreatitis-induced ADM and pancreatic reorganization in vivo.

Macrophages induce ADM of pancreatic acinar cells

To investigate whether macrophage-mediated processes can drive ADM, we cultured isolated mouse pancreatic acinar cells with activated mouse macrophages in collagen 3D primary cell culture. This ex vivo explant model for ADM is based on a previously established cell culture model in which growth factors that activate the ErbB1 EGF receptor (EGFR) have been shown to induce ADM within 6–8 d (Crawford et al., 2002; Esni et al., 2005; Means et al., 2005; Sawey et al., 2007). 3D co-culture of primary macrophages with primary acinar cells led to a 10-fold increase in ADM events, as quantified by counting of newly formed ductlike structures (Fig. 2 A). To determine whether cultured macrophages can induce similar acinar transformation, primary pancreatic acinar cells and Raw 264.7 macrophages were in vivo labeled with Vybrant dye (Fig. 2 A, pseudocolor blue [macrophages] and red [acinar cells]) and then co-cultured in 3D collagen culture. We found that Raw 264.7 macrophages induced ADM when in proximity to acinar cell clusters (Fig. 2 B). Newly formed ducts still showed red live dye staining, indicating acinar cell derivation. Quantification of ducts showed a statistically significant and ∼25-fold increase in ADM events in the presence of Raw 264.7 cells (Fig. S2 A). We then determined whether macrophages and acinar cells need direct physical contact for ADM events to occur by collagen embedding both cell types in different compartments for co-cultivation experiments (Fig. 2 C, scheme). Under such conditions, we found that Raw 264.7 macrophages do not need to be in direct contact with acinar cells to induce ADM (Fig. 2 C, right bar graph). Moreover, treatment of acinar cells in collagen culture with Raw 264.7–conditioned medium, as well as conditioned medium from WR19M.1 cells or primary activated mouse macrophages, was sufficient to induce ADM (Fig. 2, D and E), indicating that macrophage-secreted factors can induce ADM events. Treatment with TGF-α, as an inducer of EGFR signaling, served as a positive control. Duct formation correlated with decrease of

macrophage marker F4/80. Boxes in A and B indicate enlarged regions. (C) Quantitation of ADM events per field of $n = 5$ samples from B. The asterisk indicates statistical significance as determined by the Student's t test. Error bars show means ± SD. (D, top row) Immunofluorescence staining of F4/80, amylase, and DAPI in samples from FVB mice treated with control vehicle, $GdCl_3$, caerulein, or a combination, as indicated (detailed method in Materials and methods section). (second row) F4/80 channel alone in white. (third row) Immunofluorescence staining of CK-19, amylase, and DAPI. (fourth row) CK-19 channel and DAPI. Bars, 25 µm. See also Fig. S1.

Downloaded from on April 4, 2017

Published August 5, 2013

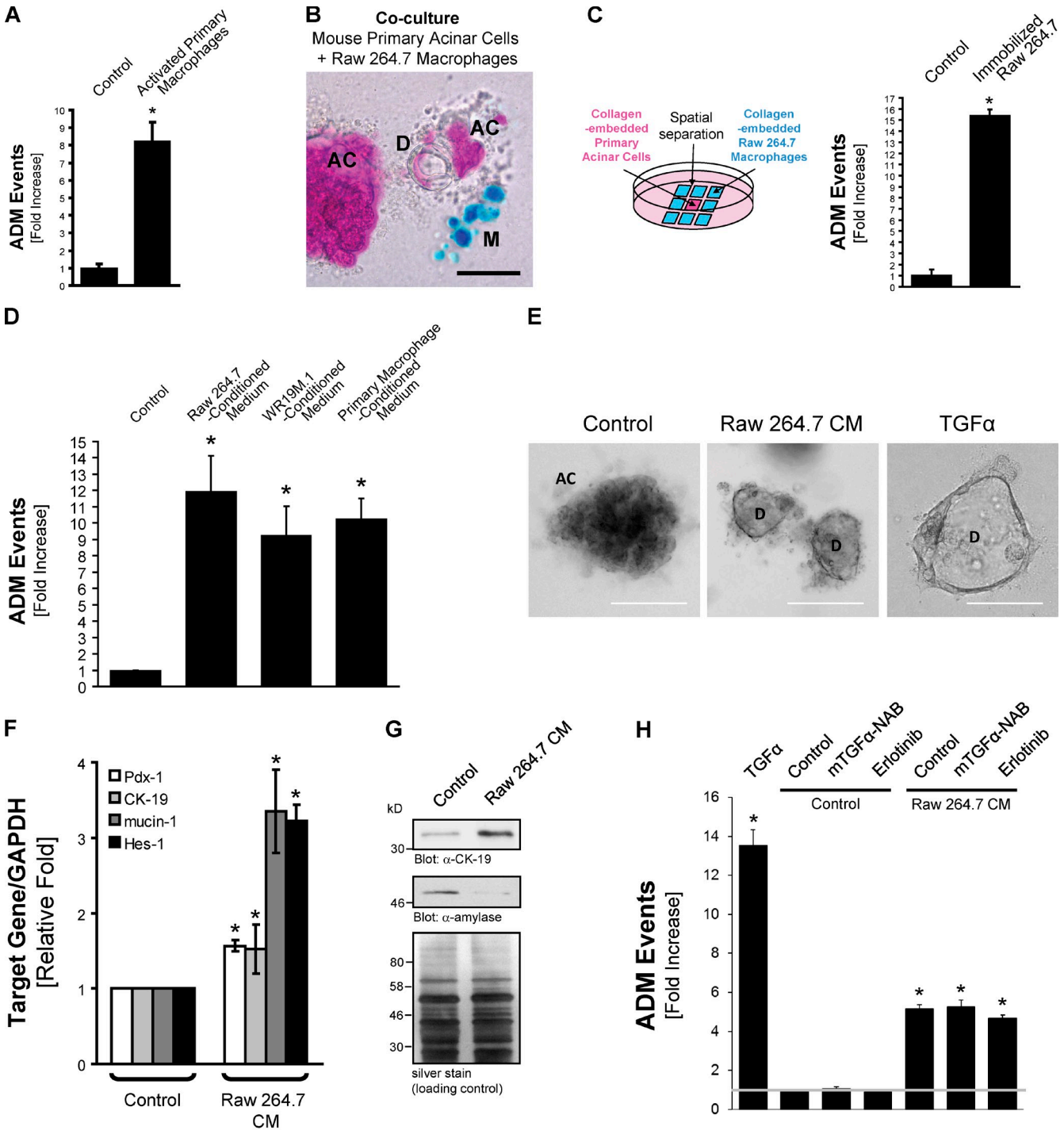

Figure 2. **Macrophages induce ADM of pancreatic acinar cells.** (A) Freshly isolated, activated mouse primary macrophages and mouse primary acinar cells were co-cultured in 3D collagen explant culture. At day 5, ADM events per well were quantified by counting. (B) Raw 264.7 and freshly isolated mouse primary acinar cells were in vivo labeled with Vybrant dyes (pseudocolors: blue, macrophages [M]; red, acinar cells [AC]) and co-cultured in 3D collagen explant culture. At day 6, co-cultures were analyzed for duct (D) formation by fluorescence microscopy (bar, 50 µm). See also Fig. S2 A. (C) Primary pancreatic acinar cells were isolated and embedded in collagen in µ-Slides (Ibidi) for cell co-cultivation (magenta area in scheme). Similarly, Raw 264.7 cells (cyan areas in scheme) were embedded in collagen (or collagen alone as a control). Cells in the collagen matrix were overlayed with Waymouth media. ADM events in the acinar cell area were determined by counting ducts. (D) Primary mouse pancreatic acinar cells were isolated and cultivated in 3D collagen explant culture in presence of Raw 264.7–, WR19M.1- or primary mouse macrophage-conditioned media, and ADM events per well were determined (graph). (E) Photos show ducts obtained (at day 5) after treatment with Raw 264.7–conditioned media as compared with untreated acinar cells and cells treated with 50 ng/ml TGF-α. Bars, 100 µm. See also Fig. S2 B. (F) Primary mouse pancreatic acinar cells were isolated and treated with Raw 264.7–conditioned media to induce ADM. At day 2, cells were isolated from the 3D collagen explant culture, and quantitative real-time PCR for indicated markers of ADM events was performed. (G) Primary mouse pancreatic acinar cells were isolated and treated with Raw 264.7–conditioned media to induce ADM. Cells were isolated from the 3D collagen explant culture, and cell lysates were analyzed for expression of the ductal marker CK-19 or the acinar marker amylase by Western blotting. Silver staining served as a loading control. (H) Primary mouse pancreatic acinar cells were isolated and treated with Raw 264.7–conditioned media to induce ADM in presence of 3 µg/ml TGF-α neutralizing antibody (mTGFα-NAB) or 1 µM Erlotinib as indicated. Treatment

Downloaded from on April 4, 2017

Published August 5, 2013

mRNA encoding the bona fide acinar cell marker amylase (Fig. S2 B) and increase in mRNA of ductal markers (Fig. 2 F) including cytokeratin-19 (CK-19) and mucin-1 (Zhu et al., 2007). Additionally, we detected an increase in expression of Pdx-1 (pancreatic duodenal homeobox-1), one of the earliest markers of embryonic endocrine and exocrine progenitor cells (Bonal and Herrera, 2008). For example, ectopic expression of Pdx-1 during development has been shown to decrease the extent of exocrine tissue and to result in the formation of immature acinar cells (Holland et al., 2002). Moreover, persistent expression of Pdx-1 in the pancreas has been shown to cause ADM (Miyatsuka et al., 2006).

We also observed up-regulation of Hes-1 (hairy and enhancer of split 1) expression (Fig. 2 F), a transcription factor that is regulated by the Notch signaling pathway and plays a key role in the development of the endocrine pancreas and maintenance of epithelial ductal structures (Sumazaki et al., 2004). Markers for ADM were further detected at the protein level, and cells showed decreased expression of the acinar marker amylase and increased expression of CK-19 when treated with Raw 264.7–conditioned media in explant culture (Fig. 2 G). Thus, our data indicate that factors secreted by macrophages induce acinar cell transdifferentiation into a ductlike phenotype. However, when compared with TGF-α, a bona fide inducer of ADM in pancreatic acinar cells, we observed that ducts formed after treatment with Raw 264.7–conditioned media were of smaller size (Fig. 2 E) and number (Fig. 2 H). Presence of an mTGF-α neutralizing antibody (NAB) as well as treatment with the EGFR inhibitor Erlotinib had no inhibitory effects on Raw 264.7–conditioned media–induced ADM (Fig. 2 H). This indicates that macrophage-conditioned media does not act through the TGF-α–EGFR signaling pathway to induce ADM.

Macrophage-secreted factors RANTES and TNF mediate ADM

Next, we analyzed Raw 264.7–, WR19M.1-, or primary mouse macrophage-conditioned media for macrophage-secreted cytokines using mouse cytokine profiler arrays. Out of 40 cytokines tested (Fig. 3 A and Fig. S3 A), eight were strongly abundant in the conditioned media but not in control media. These included granulocyte colony-stimulating factor (G-CSF; at B5/6), IP-10/CXCL10/CRG-2 (at D1/2), junctional epithelium (JE)/CCL2/MCP-1 (at D9/10), MIP-1α/CCL3 (at D15/16), MIP-1β/CCL4 (at D17/18), MIP-2 (at D19/20), RANTES/CCL5 (at D21/22), and TNF (at E5/6). Of these cytokines, only TNF and RANTES induced pronounced ADM events, as judged by analysis of newly formed ducts (approximately threefold increase as compared with untreated controls) in our explant culture assays (Fig. 3 B). We detected TNF at 107 ± 15 pg/ml and RANTES at 842 ± 4 pg/ml in conditioned media from primary macrophages, TNF at 6.5 ± 0.8 pg/ml and RANTES at 83 ± 5 pg/ml in conditioned media from WR19M.1 cells, and TNF at 50 ± 13 pg/ml and RANTES at 841 ± 4.4 pg/ml in conditioned media from Raw 264.7 cells.

When applied to pancreatic acinar cell explant culture, both cytokines were less potent inducers of ADM as conditioned media, and the treatment of acinar cells with all combinations of identified cytokines did not lead to additive effects (unpublished data). This suggests that additional, yet unidentified, factors in the conditioned media may also be required to obtain a more effective transdifferentiation of acinar cells. Moreover, when we blocked signaling of TNF or RANTES in pancreatic explant culture by using NABs, both significantly decreased Raw 264.7–conditioned media–induced ADM (Fig. 3 C). However, combination of both NABs (unpublished data) had no additive effects, suggesting that both cytokines may use the same mechanisms.

To test whether TNF and RANTES can be detected in human pancreatitis, we analyzed their occurrence in samples of human pancreatitis or normal pancreas (Fig. 3, D and E). Both cytokines were detected in acinar clusters undergoing ADM but not in normal pancreas. Concentrations of both cytokines were also increased in pancreatic cyst fluid in patient samples of pancreatitis, with an approximately threefold (TNF) or 3.5-fold (RANTES) increase as compared with pancreatic juice from control patients (Fig. S3 B).

RANTES and TNF induce acinar cell transdifferentiation through NF-κB

A common feature of both cytokines, TNF and RANTES, is that they can activate the transcription factor NF-κB, which is involved in the regulation of many inflammatory processes (Ben-Neriah and Karin, 2011). Constitutive NF-κB expression and activity were described as some of the earliest events distinguishing human tissue samples of normal pancreas from such of pancreatitis and pancreatic adenocarcinoma (Gukovsky et al., 1998; Wang et al., 1999; Chandler et al., 2004). However, a role for this transcription factor in regulating the ADM process has not been implicated previously. Therefore, we tested whether NF-κB can be induced by macrophage-conditioned media. We introduced an NF-κB–luciferase reporter into acinar cells using an adenoviral transduction system. Increased NF-κB activity was measured in response to Raw 264.7–conditioned media (Fig. 4 A). We then used two inhibitors for IκB kinase, SC514 and BMS345541, to identify a role for NF-κB in Raw 264.7–conditioned media–induced ADM. Both inhibitors effectively blocked Raw 264.7–conditioned media–induced ADM, whereby BMS345541 was more effective than SC514 (Fig. 4 B).

A key event in canonical NF-κB signaling is the down-regulation of IκBα. Treatment of primary acinar cells with conditioned media, as well as TNF and RANTES, led to the down-regulation of the NF-κB inhibitory protein IκBα over a time range of 24–96 h (Fig. 4 C, shown is the IκBα status at 24 h of stimulation). Adenoviral infection of acinar cells with a superdominant IκBα (IκBα.SD and IκBα.S32A.S36A;

with 50 ng/ml TGF-α served as a comparison to conditioned media. At day 5, ADM events per well were quantified by counting. The gray line represents onefold ADM events. In the experiments depicted in A, C, D, F, and H, bar graphs show means ± SD of $n = 3$ experiments. The asterisk indicates statistical significance as determined by the Student's *t* test. All experiments depicted have been repeated with similar results at least three times.

Downloaded from on April 4, 2017

Published August 5, 2013

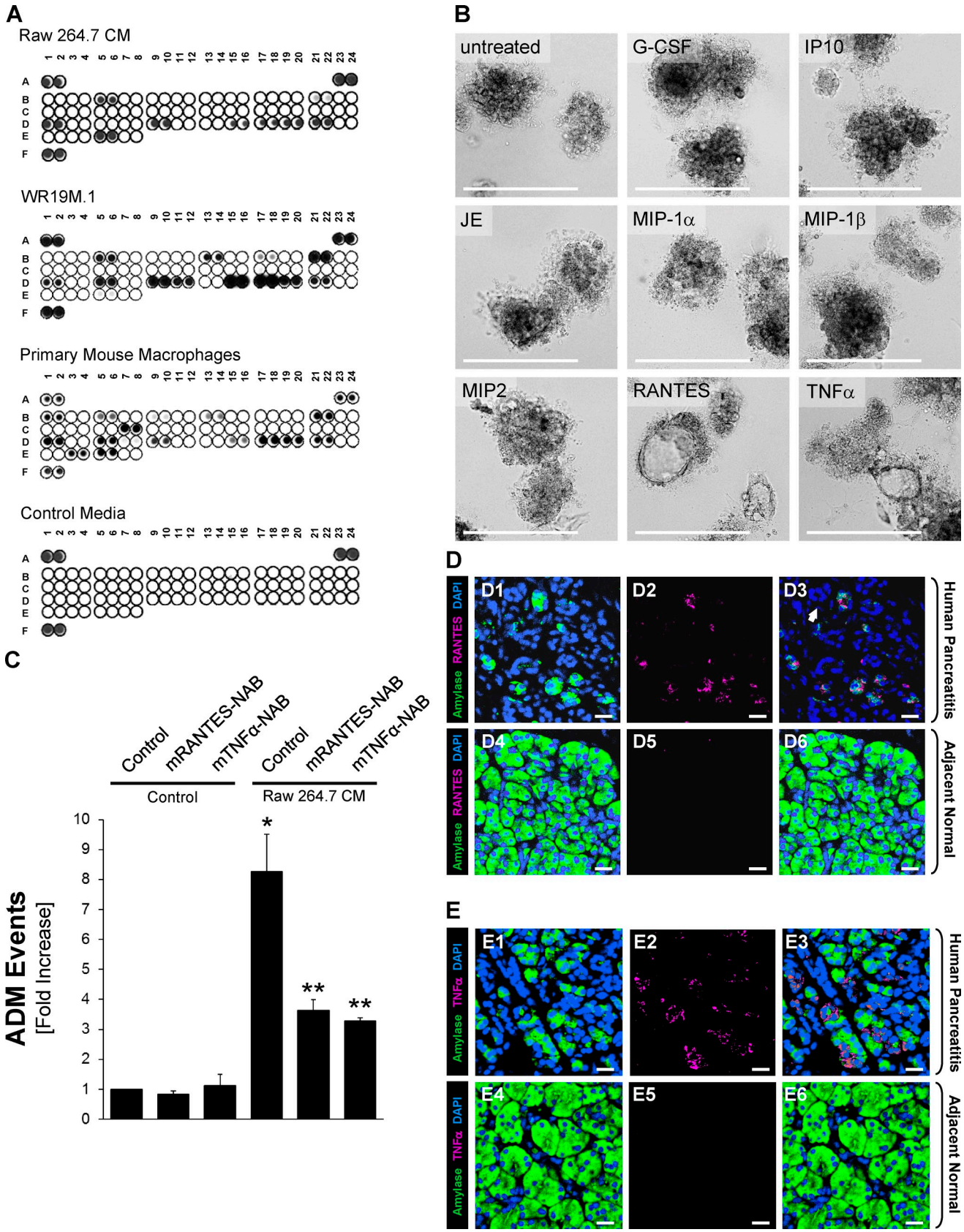

Figure 3. **Macrophage-secreted factors RANTES and TNF mediate ADM.** (A) Conditioned media from Raw 264.7, WR19M.1, activated primary mouse macrophages, or control media (bottom) were subjected to a mouse cytokine profiler array allowing the detection of 40 different cytokines (see table in Fig. S3 A for cytokine identity and position on the array; A1/2, A23/24, and F1/2 contain positive controls, and F23/F24 contains negative controls). (B) Mouse primary acinar cells were co-cultured in 3D collagen explant culture in the presence of the cytokines (G-CSF, IP-10, JE, MIP-1α, MIP-1β, MIP2,

Downloaded from on April 4, 2017

Published August 5, 2013

Lee et al., 1997) before 3D explant culture effectively blocked the induction of ADM by Raw 264.7–conditioned media (Fig. 4 D and Fig. S4, A and B), TNF, or RANTES (Fig. 4 E). This indicates that canonical activation of NF-κB contributes to ADM events. To test whether NF-κB can drive ADM, we infected acinar cells with an adenovirus encoding NF-κB1/p105 (p50 of the mature NF-κB) before seeding them in 3D explant culture. We found that the expression of NF-κB/p105 in acinar cells is sufficient to mediate their transdifferentiation to ductlike cells (Fig. 4 F). This was confirmed by quantitative PCR analysis showing an increase in expression of the ductal markers CK-19 and mucin-1 as well as Pdx-1 when NF-κB is expressed (Fig. 4 G). Furthermore, we observed down-regulation of mouse Mist-1 (muscle intestine and stomach expression 1), a gene that is necessary for the complete maturation and proper function of acinar cells and maintains acinar cell identity (Pin et al., 2001). This further indicates acinar cell dedifferentiation.

The NF-κB target gene MMP-9 drives acinar cell transdifferentiation in explant culture and in vivo

To identify target genes for NF-κB in acinar cells, we then performed quantitative real-time PCR target arrays and compared control acinar cells to NF-κB–transdifferentiated ductlike cells of pancreatic explant cultures from three different mice. Genes targeted by NF-κB that are up- or down-regulated at least twofold were identified (Fig. S5, volcano blot and complete list of genes analyzed). In acinar cells, the expression of NF-κB orchestrated the induction of genes involved in all aspects of the reprogramming process. This included the down-regulation of proapoptotic genes such as *Egr-2* (5.6-fold), and up-regulation of antiapoptotic genes such as *AKT1* (2.7-fold), *Bcl-XL* (2.7-fold), *Bcl2A1* (threefold), *COX-2* (fourfold), and *MKK6* (3.7-fold). We also detected up-regulation of genes promoting cell cycle progression and proliferation such as *CDK1* (3.6-fold) and *CCND1* (7.6-fold) and of genes encoding growth factors such as *PDGFb* (2.8-fold). We further detected substantial up-regulation of *Csf3* (19-fold) and *Csf2* (70-fold), indicating an important role for these colony-stimulating factors in the ADM process. Moreover, induction of *CCL5* encoding RANTES (26-fold) indicates a positive feedback loop to potentiate the signaling.

Effective ADM also requires the expression of proteases of the disintegrin, ADAM (a disintegrin and a metalloprotease) protease, or MMP families (Crawford et al., 2002; Ringel et al., 2006; Sawey et al., 2007; Fukuda et al., 2011). Interestingly, one top hit in our assay to identify NF-κB target genes in acinar cells was MMP-9 (58-fold induction and $P < 0.05$). Human pancreatic cancers express high levels of MMP-9 (Gress et al., 1995), and its expression is essential to angiogenesis and tumor growth of orthotopic pancreatic tumors (Nakamura et al., 2007). Increased MMP-9 expression already can be detected in PanIN lesions (Segara et al., 2005). However, a crucial role for this isoform in the ADM process so far was not attributed. Because our initial array was restricted to MMP-9, we performed additional quantitative real-time PCR assays to determine the subset of MMPs that may be involved in NF-κB–mediated ADM. With this assay, in cells undergoing ADM in response to NF-κB1, we detected an ∼500-fold increased expression of MMP-9, whereas the expression of MMP-3, MMP-7, and MMP-13 was increased twofold, and MMP-10 was increased approximately eightfold (Fig. 5 A). The increased expression of MMP-9 led to secretion of active MMP-9 as shown with gelatin zymography of supernatants of transdifferentiating acinar cells (Fig. 5 B).

We next tested whether addition of purified, active MMP-9 to acinar cells when embedded in 3D explant culture can drive ADM (Fig. 5 C). We observed an approximately twofold increase in ADM events, underlining the importance of MMP-9 in this process. However, the moderate increase in ADM events in response to addition of MMP-9 clearly indicates that additional molecules, either regulated by NF-κB–dependent or –independent genes, are necessary for more pronounced effects on ADM. This is not surprising given the complexity of this transdifferentiation process. Nevertheless, treatment of acinar cells with the MMP inhibitor GM6001 effectively blocked Raw 264.7–conditioned media–, TNF-, and RANTES-induced acinar cell transformation, indicating the importance of MMPs in regulating ADM (Fig. 5, D and E). Similarly, GM6001 blocked basal- and NF-κB–induced duct formation in 3D explant culture (Fig. 5 F), without impacting cell survival (not depicted).

Our findings directly correlate with the in vivo situation because in the caerulein animal model for pancreatitis, MMP-9 was strongly expressed in inflamed pancreas but not when macrophages were suppressed with $GdCl_3$- or in control-treated mice (Fig. 6 A). When applied in vivo, the MMP inhibitor GM6001 effectively blocked pancreatitis-induced acinar cell metaplasia (Fig. 6, B and C). To determine whether such MMP signaling also occurs in human pancreatitis, we compared samples of human pancreatitis to normal pancreatic tissue for MMP-9 expression. We found increased expression of this metalloproteinase in pancreata of pancreatitis patients in areas that undergo ADM but not in adjacent normal pancreatic tissue (Fig. 6 D).

Downloaded from on April 4, 2017

RANTES, or TNF; all at 50 ng/ml) that were specifically identified in conditioned media from macrophages. Shown is a representative picture of each condition showing either acinar or ADM clusters. (C) Primary mouse pancreatic acinar cells were isolated and treated with Raw 264.7–conditioned media to induce ADM in the presence of neutralizing antibodies (NAB) for 0.5 µg/ml mRANTES and 3 µg/ml mTNF-α as indicated. At day 5, ADM events per well were quantified by counting. The single asterisk indicates statistical significance as compared with control determined by the Student's *t* test. Double asterisks indicate statistical significance as compared with control and as compared with Raw 264.7–conditioned medium–induced ADM as determined by the Student's *t* test. Bar graph shows means ± SD of $n = 3$ experiments. (D) Immunofluorescence staining of amylase, RANTES, and DAPI in human pancreas tissues containing a pancreatitis-affected area (top row) and adjacent normal area (bottom row). (left, D1 and D4) Amylase + DAPI; (middle, D2 and D5) RANTES; (right, D3 and D6) merged images containing amylase, DAPI, and RANTES. (E) Immunofluorescence staining of amylase, TNF, and DAPI in human pancreas tissues containing areas affected by pancreatitis (top row) or adjacent normal area (bottom row). (left, E1 and E4) Amylase + DAPI; (middle, E2 and E5) TNF; (right, E3 and E6) merged images containing amylase, TNF, and DAPI. See also Fig. S3 B. All experiments depicted have been repeated with similar results at least three times. Bars: (B) 200 µm; (D and E) 20 µm.

Published August 5, 2013

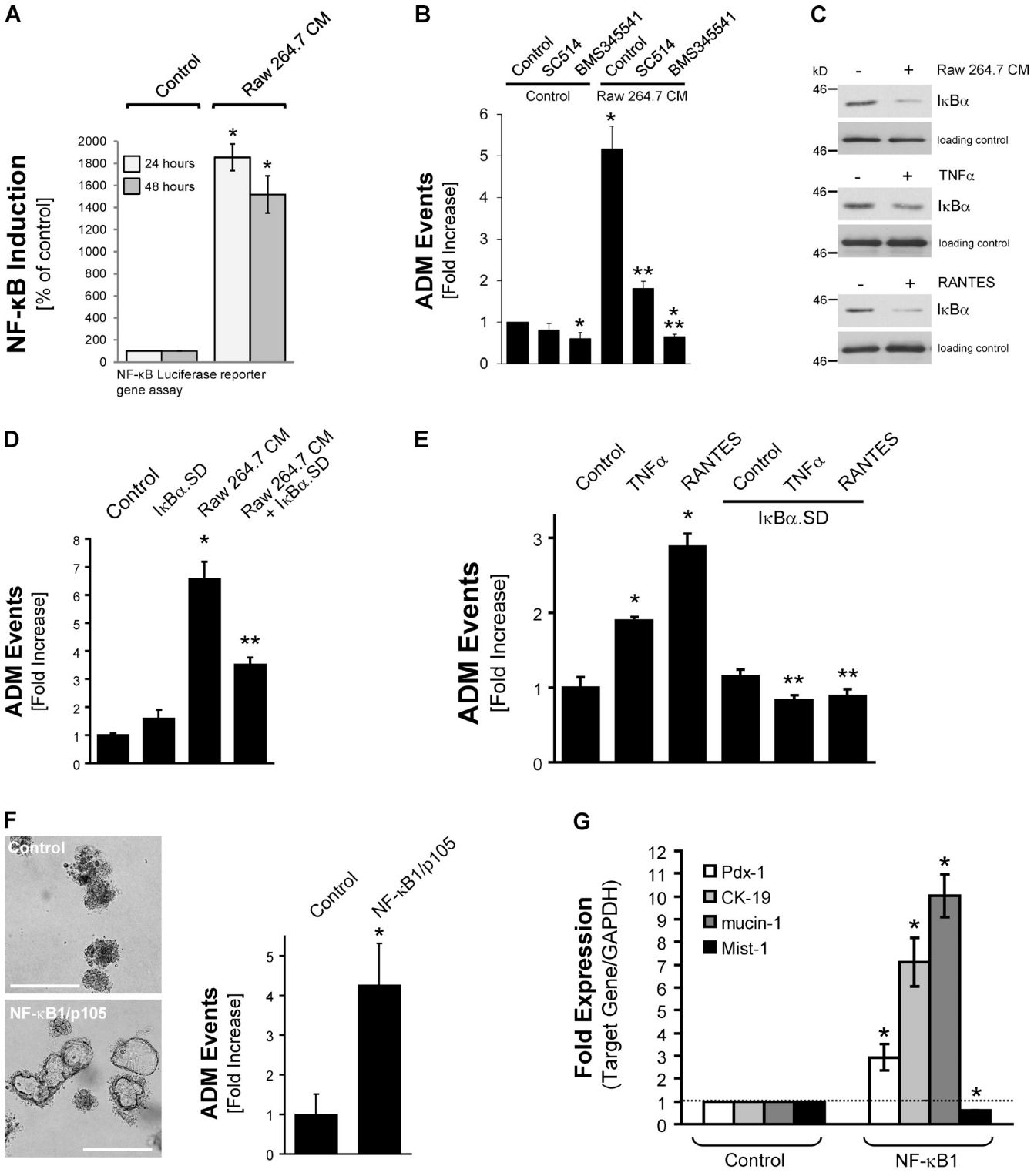

Figure 4. **RANTES and TNF induce acinar cell transdifferentiation through NF-κB.** (A) Primary mouse pancreatic acinar cells were isolated and infected with adenovirus carrying an NF-κB–luciferase reporter. Cells were treated with control or Raw 264.7–conditioned media for 24 and 48 h. NF-κB promoter activity was determined by measuring luciferase activity. NF-κB induction as compared with control (set to 100%) is shown. The asterisk indicates statistical significance as compared with control. (B) Primary mouse pancreatic acinar cells were isolated and treated with Raw 264.7–conditioned media in the presence of 25 µM SC514 or 1 µM BMS345541 as indicated. ADM events per well were quantified by counting ducts formed. (C) Primary mouse pancreatic acinar cells were isolated and treated with Raw 264.7–conditioned media, 50 ng/ml TNF, or 50 ng/ml RANTES as indicated for 24 h. Cells were lysed and analyzed by Western blotting for IκBα degradation using an α-IκBα antibody. (D) Primary mouse pancreatic acinar cells were isolated and infected with control virus or adenovirus to express superdominant IκBα (IκBα.SD). Cells were then cultivated in 3D collagen explant culture in presence of Raw 264.7–conditioned media or control media as indicated. ADM events per well were quantified by counting. See also Fig. S4. (E) Primary mouse pancreatic acinar cells were isolated and infected with control virus or adenovirus to express superdominant IκBα (IκBα.SD). Cells were then cultivated in 3D collagen explant culture in presence of 50 ng/ml TNF or 50 ng/ml RANTES as indicated. ADM events per well were quantified by counting. (F) Primary

Downloaded from on April 4, 2017

Published August 5, 2013

Together, our data indicate that macrophage-induced expression of MMPs in acinar cells is an important mediator of the ADM process in pancreatitis.

Discussion

Many cancers can arise from sites of chronic irritation, infection, or inflammation (Coussens and Werb, 2002). Inflammation of the pancreas has been recognized as a risk factor for pancreatic cancer, but the roles of macrophage infiltration in the pancreas on processes leading to altered pancreas morphology and eventually pancreatic cancer are not well understood. In response to many insults, pancreatic acinar cells can undergo a reprogramming event that induces transdifferentiation to a ductlike phenotype. In the context of oncogenic stimulation, resulting ductlike cells can further progress to pancreatic adenocarcinoma (Guerra et al., 2007, 2011). We here provide evidence that macrophages infiltrating the pancreas can drive this transdifferentiation process and also provide insight into the mechanisms they use.

Our results demonstrate that the macrophage-secreted proinflammatory cytokines RANTES and TNF, both previously not directly implicated in this process, are inducers of acinar cell dedifferentiation and metaplasia to a ductal phenotype (Fig. 3). Although little is known about the role of RANTES in pancreatic cancer, TNF was shown to be synthesized not only by macrophages but also by inflamed pancreatic acinar cells and to have paracrine effects in both pancreatitis and PDAC (Chu et al., 2007). Both cytokines were less potent inducers of ADM as macrophage-conditioned media (compare Fig. 2 D with Fig. 4 E), and the treatment of acinar cells with combinations of both cytokines did not lead to additive effects (not depicted). This suggests that additional yet unidentified factors in the conditioned media may also be required to obtain a more effective transdifferentiation of acinar cells. Also, when compared with TGF-α, as a bona fide inducer of ADM in pancreatic acinar cells, we observed that ducts formed after treatment with Raw 264.7–conditioned media were of smaller size and number (Fig. 2, E and H). Moreover, macrophage-induced ductal structures did not continuously grow over time as it was previously shown for TGF-α–induced structures. This indicates that macrophages, although initiating acinar cell transdifferentiation, do not activate additional signaling pathways, further driving proliferation of the resulting ductal cells. Key events crucial for further progression may involve the loss of LKB1 or combination of oncogenic K-ras with deletion of p16/p19 as it was recently shown by Lo et al. (2012).

Our data suggest that macrophages use TNF and RANTES to induce the activation of the transcription factor NF-κB and drive ADM in acinar cells (Fig. 4). Additionally, expression of NF-κB1 in acinar cells can drive ADM in our ex vivo explant culture (Fig. 4, F and G). A role for this transcription factor in regulating the ADM process has not been implicated previously; however, constitutive NF-κB expression and activity were described as some of the earliest events distinguishing human tissue samples of a normal pancreas from such of pancreatitis and pancreatic adenocarcinoma (Gukovsky et al., 1998; Wang et al., 1999; Chandler et al., 2004). Recently, Daniluk et al. (2012) showed that in the presence of oncogenic K-ras, inflammatory stimuli via NF-κB initiate a positive feedback loop that further amplifies Ras activity to pathological levels. This led to prolonged Ras signaling and precancerous pancreatic lesions (PanINs) in mice expressing oncogenic K-ras but not in wild-type mice (Daniluk et al., 2012). We obtained data complementary to this finding because macrophage depletion in $p48^{cre}$/LSL-KrasG12D mice dramatically reduced ADM and formation of PanIN lesions (Fig. S1, D and E). This further underlines the importance of macrophages in contributing to ADM and eventually progression to PanIN lesions. Thus our data implicate that targeting NF-κB could be an effective strategy not only to target pancreatitis but also precursor lesions that could lead to the development of PDAC.

Isolated acinar cells in explant culture are quiescent and undergo cell death after several days in culture, when not stimulated for transdifferentiation. In contrast, after initiation of the ADM process, cells become proliferative and acquire properties to form ducts (Puri and Hebrok, 2010). NF-κB target genes identified in acinar cells (Fig. S5) are involved in all aspects of the reprogramming process. We observed up-regulation of genes that clearly are linked to antiapoptotic signaling. These include *AKT1* (2.7-fold), *Bcl-XL* (2.7-fold), *Bcl2A1* (threefold), *COX-2* (fourfold), and *MKK6* (3.7-fold). Of the aforementioned genes, *COX-2* may be of particular importance because it also was shown to contribute to accelerated progression of $K\text{-}ras^{G12D}$–induced PanIN lesions (Funahashi et al., 2007). COX-2 is up-regulated in inflamed acinar components of chronic pancreatitis in PanIN and in PDAC (Tucker et al., 1999; Schlosser et al., 2002; Albazaz et al., 2005). Other genes up-regulated by NF-κB are well-known inducers of cell cycle progression and proliferation. These include *CDK1* (3.6-fold) and *CCND1* (7.6-fold). We further detected substantial up-regulation of *Csf3* (19-fold) and *Csf2* (70-fold), indicating an important role for these colony-stimulating factors in survival and proliferation of acinar cells. Finally, induction of *CCL5* encoding RANTES (26-fold) indicates a positive feedback loop to potentiate the signaling. Moreover, secretion of RANTES may recruit additional inflammatory cells.

Although the genes listed in the previous paragraph mainly are involved in acinar cell survival or inducing their proliferation, effective ADM also requires the expression of proteases of the disintegrin, ADAM protease, or MMP families (Crawford

mouse pancreatic acinar cells were isolated and infected with control virus or adenovirus to express NF-κB1/p105. Cells were then cultivated in 3D collagen explant culture. Representative photographs of the cells in 3D culture are shown (left side), and ADM events per well were quantified by counting (right side). Bars, 200 µm. (G) Primary mouse pancreatic acinar cells infected with control virus or adenovirus to express NF-κB1/p105 were isolated from 3D collagen explant culture at day 3. Quantitative PCR for the indicated markers of ADM events was performed. Dotted line represents onefold expression. In the experiments depicted in A, B, and D–G, bar graphs show means ± SD of $n = 3$ experiments. The asterisks indicate statistical significance as determined by the Student's *t* test (single asterisks show statistical significance relative to the control; double asterisks show statistical significance relative to the stimulus). All experiments depicted have been repeated with similar results at least three times. CM, conditioned media.

Downloaded from on April 4, 2017

Published August 5, 2013

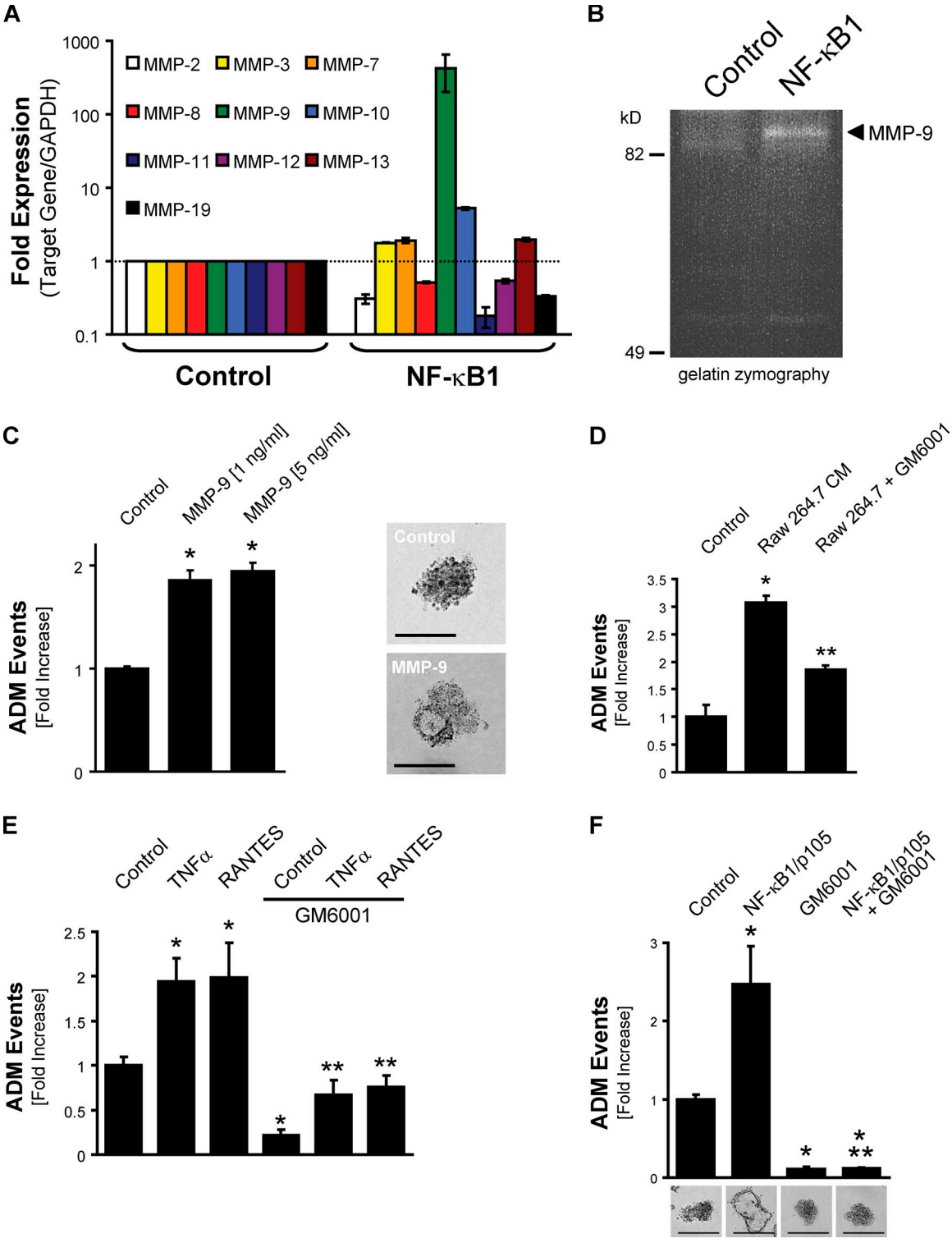

Figure 5. **NF-κB drives acinar cell transdifferentiation through MMP-9.** (A) Primary mouse pancreatic acinar cells that were infected with control virus or adenovirus to express NF-κB1/p105 were isolated at day 6 from 3D collagen explant culture. Quantitative real-time PCR for the indicated MMPs was performed. Dotted line represents onefold expression. Bar graphs show means ± SD of $n = 3$ experiments. (B) Gelatin zymography with supernatants from primary mouse pancreatic acinar cells that were infected with control virus or adenovirus to express NF-κB1/p105 and underwent ADM in 3D collagen explant culture. The arrow indicates active MMP-9. (C) Primary mouse pancreatic acinar cells were isolated and cultivated in 3D collagen explant culture in presence of recombinant MMP-9 (1 and 5 ng/ml). (left) At day 5, ADM events per well were quantified by counting. (right) Representative photographs of the cells in 3D culture are shown. Bars, 100 µm. (D) Primary mouse pancreatic acinar cells were isolated and cultivated in 3D collagen explant culture in presence of Raw 264.7–conditioned media and the MMP inhibitor GM6001 (2 µM) as indicated. At day 5, ADM events per well were quantified by counting. (E) Primary mouse pancreatic acinar cells were isolated and cultivated in 3D collagen explant culture in the presence of the MMP inhibitor GM6001 (2 µM), 50 ng/ml TNF, or 50 ng/ml RANTES as indicated. At day 5, ADM events per well were quantified by counting. (F) Primary mouse pancreatic acinar cells were isolated, infected with control virus or adenovirus to express NF-κB1/p105, and cultivated in 3D collagen explant culture in the presence of the MMP inhibitor GM6001 (2 µM). (top) At day 7, ADM events per well were quantified by counting. (bottom) Representative photographs of the cells in 3D culture

Downloaded from on April 4, 2017

Published August 5, 2013

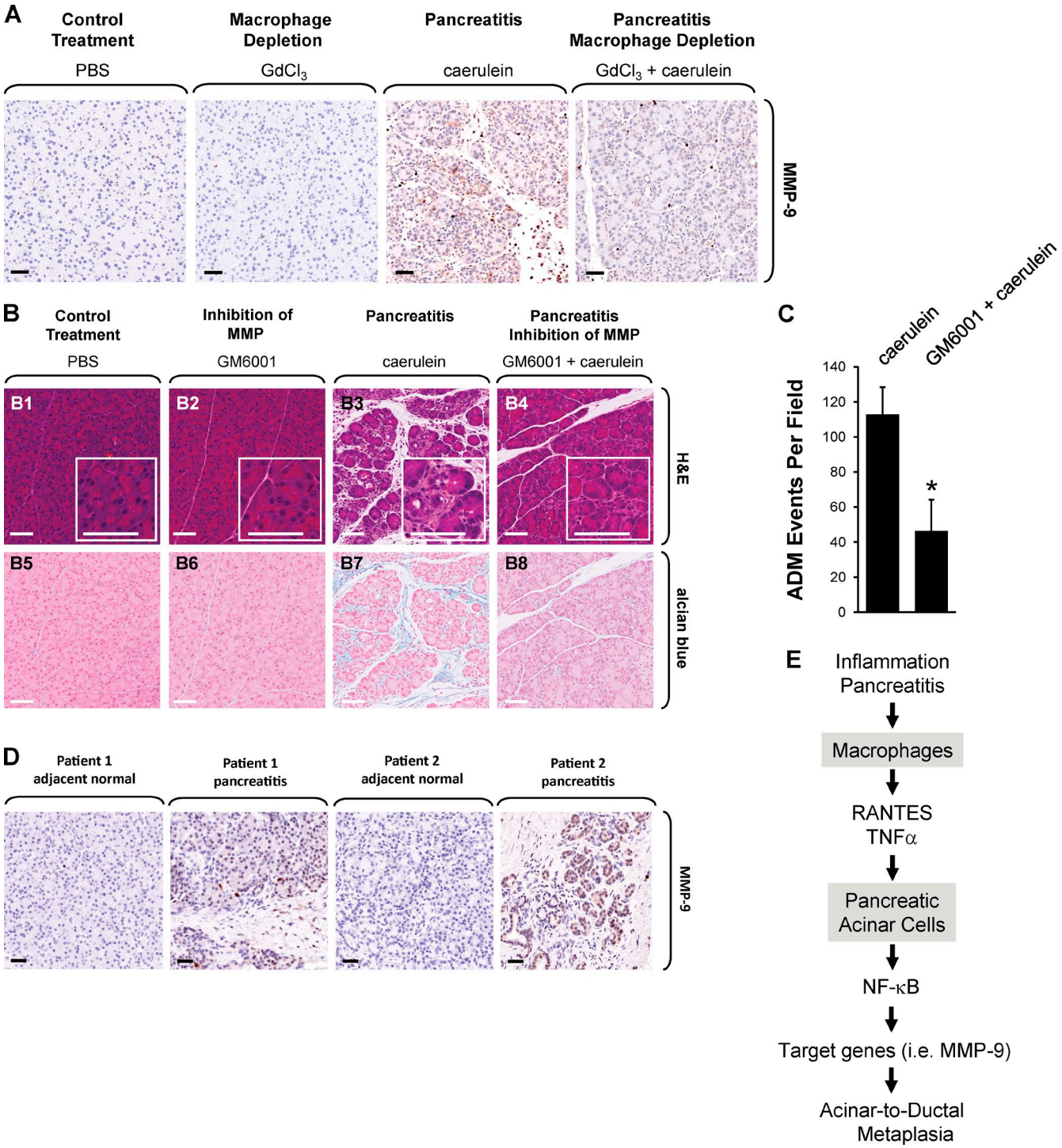

Figure 6. **MMPs contribute to ADM in vivo.** (A) FVB mice were treated with control vehicle, $GdCl_3$, caerulein, or a combination, as indicated. Pancreata were harvested and IHC stained for MMP-9 expression. (B) FVB mice were treated with control vehicle, GM6001, caerulein, or a combination, as indicated (detailed method in the Materials and methods section). Pancreata were harvested and IHC stained with H&E or Alcian blue. Boxes show the sample at a higher magnification. (C) Quantitation of ADM events per field of $n = 5$ samples from B. Bar graphs show means ± SD. The asterisk indicates statistical significance as determined by the Student's *t* test. (D) MMP-9 expression in human pancreas tissues containing areas that are affected by pancreatitis and the adjacent normal regions. (E) Schematic of the proposed signaling events induced by macrophages after pancreatic inflammation. Our data suggest that macrophage-secreted inflammatory cytokines, such as RANTES and TNF, induce NF-κB in pancreatic acinar cells and that the target genes for this transcription factor can drive ADM. Bars, 100 μm.

are shown. Bars, 200 μm. In the experiments depicted in A and C–F, bar graphs show means ± SD of $n = 3$ experiments. The asterisks indicate statistical significance as determined by the Student's *t* test (single asterisks show statistical significance relative to the control; double asterisks show statistical significance relative to the stimulus). All experiments depicted have been repeated with similar results at least three times.

Downloaded from on April 4, 2017

Published August 5, 2013

et al., 2002; Ringel et al., 2006; Sawey et al., 2007; Fukuda et al., 2011; Ardito et al., 2012). MMPs were associated with tumor initiation and progression processes by targeting not only ECM components but also non-ECM substrates (Coussens and Werb, 2002). In pancreatic cancer, evidence from mouse genetics demonstrated that MMPs not only target ECM substrates but also contribute to multiple stages of pancreatic tumor progression including tumor growth (Sawey et al., 2007). For example, MMP-3 and MMP-7 are required for Notch activation, leading to dedifferentiation of acinar cells to nestin-positive transitional cells (Sawey et al., 2007). Additionally, MMP-7 was shown to contribute to initiation and progression of PDAC (Fukuda et al., 2011). Interestingly, one top hit in our assay to identify NF-κB target genes in acinar cells was MMP-9 (58-fold induction and $P < 0.05$; Fig. 5 and Fig. S5). MMP-9 can be expressed and secreted by macrophages, stromal cells, or tumor cells (Storz et al., 2009). Human pancreatic cancers express high levels of MMP-9 (Gress et al., 1995), and its expression is essential to angiogenesis and tumor growth of orthotopic pancreatic tumors (Nakamura et al., 2007). Increased MMP-9 expression already can be detected in PanIN lesions (Segara et al., 2005). When expressed by acinar cells or when recombinant active protein was added to the media, MMP-9 was capable to drive ADM, indicating that it is a substantial contributor to the transdifferentiation process (Fig. 5 C). The MMP inhibitor GM6001 effectively blocked pancreatitis-induced ADM in vivo in our caerulein mouse model (Fig. 6 B). A role for this isoform in the ADM process was not attributed previously, and it remains to be determined whether MMP-9, like MMP-7, can cleave and activate Notch to drive the ADM process.

Collectively, we provide evidence for a mechanism of how inflammation of the pancreas can induce ADM and thus provide a setup for tumor initiation. We further establish macrophage-secreted cytokines as substantial drivers of ADM and show that they mediate their effects on acinar cells through NF-κB and NF-κB–induced target genes. Because high NF-κB levels were observed in pancreatic cancer, but not in normal acinar tissue, our data provide a mechanistic link between acinar cell reprogramming and potential development of pancreatic cancer. The identification of MMPs as a target group for NF-κB signaling that drives ADM suggests that MMP inhibitors may be efficiently applied to block pancreatitis-induced ADM in therapy.

Materials and methods

Cell lines, antibodies, viral constructs, and reagents

Raw 264.7 and WR19M.1 macrophage cells (ATCC) were maintained in DMEM (high glucose) containing 10% FBS or 10% horse serum, respectively, with 100 U/ml penicillin/streptomycin in a 37°C incubator supplemented with 5% CO_2. To obtain Raw 264.7– or WR19M.1-conditioned media, 3×10^6 cells per 10-cm dish were grown in media used for 3D collagen explant culture (Waymouth media plus supplements; see Isolation of primary pancreatic acinar cells and macrophages section), and supernatants were collected. Conditioned media was freshly prepared for each experiment. The antiamylase antibody was obtained from Sigma-Aldrich; anti-F4/80/EMR1, anti-CD3, anti–smooth muscle antibody, anti-EGFR, anti-TNF, anti-RANTES, and an NAB for mTGF-α were obtained from Abcam; anti–CK-19 antibody (for Western blotting) was purchased from Leica; anti–CK-19 antibody (for immunofluorescence) was obtained from Santa Cruz Biotechnology, Inc.; and the anti-IκBα antibody was obtained from Cell Signaling Technology. The Ly6B.2 antibody was purchased from AbD Serotec, the anti–Claudin-18 antibody was purchased from Invitrogen, the NAB for mRANTES was obtained from R&D Systems, and the NAB for mTNF-α was obtained from eBioscience. Adenovirus to express IκBα.S32A. S36A and NF-κB1/p105 or the NF-κB–luciferase reporter was purchased from Vector Laboratories. In all experiments, virus was used at 10^7 ifu/ml. Recombinant murine G-CSF, IP10, JE, MIP-1α, MIP-1β, MIP2, RANTES, and TNF were purchased from PeproTech. Recombinant human MMP-9 and recombinant TGF-α were obtained from R&D Systems. Soybean trypsin inhibitor was obtained from Affymetrix, and collagenase I was purchased from EMD. Rat tail collagen I was obtained from BD. GM6001, BMS 345541, and SC514 were obtained from EMD Millipore. Erlotinib was purchased from LC Laboratories. Caerulein, gadolinium chloride hexahydrate, and dexamethasone were obtained from Sigma-Aldrich. Other antibodies and reagents used are described in the specific experiment sections.

Animals and treatment

BALB/c and FVB (friend virus B type) mice for isolation of primary pancreatic acinar cells were purchased from Harlan Laboratories. To determine the effects of macrophages or MMPs on pancreatitis-induced ADM, 7-wk-old FVB mice were intravenously injected with either PBS (control), $GdCl_3$ (10 mg/kg body weight, every 2 d for 1 wk before caerulein treatment), or GM6001 (100 mg/kg body weight, 30 min before caerulein treatment). To induce pancreatitis, caerulein (75 µg/kg body weight) was intraperitoneally injected once per hour for a time span of 8 h, 2 d in a row (Morris et al., 2010a; Fukuda et al., 2011). Phosphate saline solution was used as a control. Pancreata were harvested 1 d after caerulein treatment. All animal experiments were approved by the Mayo Clinic Institutional Animal Care and Use Committee and were performed in accordance with relevant institutional and national guidelines and regulations.

Isolation of primary pancreatic acinar cells and macrophages

The pancreas was removed, washed twice with ice-cold HBSS media, minced into 1–5-mm pieces, and digested with collagenase I (37°C with shaker). The collagen digestion was stopped by addition of an equal volume of ice-cold HBSS media containing 5% FBS. The digested pancreatic pieces were washed twice with HBSS media containing 5% FBS and pipetted through a 500-µm mesh and then a 105-µm mesh. The supernatant of this cell suspension containing acinar cells was dropwise added to the top of 20 ml HBSS containing 30% FBS. Acinar cells were then pelleted (1,000 rpm for 2 min at 4°C) and resuspended in 10 ml Waymouth complete media (1% FBS, 0.1 mg/ml trypsin inhibitor, and 1 µg/ml dexamethasone). Primary murine macrophages were isolated as previously described (Necela et al., 2008). In brief, mice were intraperitoneally injected with 2 ml of 3–5% aged thioglycollate solution. On day 5 after injection, peritoneal macrophages were collected through a single injection of 10 ml RPMI 1640 containing 10% FBS into the peritoneal cavity and subsequent withdrawal. The peritoneal exudate was centrifuged and washed with RPMI 1640 media containing 10% FBS before plating onto tissue-culture dishes. After 1 h in a 37°C incubator supplemented with 5% CO_2, cells were vigorously washed with PBS for three times to remove nonadherent macrophages.

3D collagen explant culture of pancreatic acinar cells

Cell culture plates were coated with collagen I in Waymouth media without supplements. Freshly isolated primary pancreatic acinar cells were added as a mixture with collagen I/Waymouth media on the top of this layer (3D on-top method). Furthermore, Waymouth complete media was added on top of the cell/gel mixture and replaced the following day and then every other day. When inhibitors, peptides, or proteins were added, the compound of interest was added to both, and the cell/gel mixture and the media were added on top. To express proteins using adenovirus, acinar cells were infected with adenovirus of interest and incubated for 3–5 h before embedding in the collagen I/Waymouth media mixture. At day 6 or 7 (dependent on time course of duct formation), numbers of ducts were counted under a microscope, and photos were taken to document structures.

Immunohistochemistry (IHC)

Slides were deparaffinized (1 h at 60°C), dewaxed in xylene (five times for 4 min), and gradually rehydrated with ethanol (100, 95, and 75%, each two times for 3 min). The rehydrated samples were rinsed in water and subjected to antigen retrieval in 10 mM sodium citrate buffer, pH 6.0, as described by the manufacturer (Dako). Slides were treated with 3% H_2O_2 (5 min) to reduce endogenous peroxidase activity, washed with PBS containing 0.5% Tween 20, and blocked with protein block serum-free solution (Dako) for 5 min at room temperature. Samples were stained with hematoxylin and eosin (H&E), Alcian blue, anti–MMP-9 antibody (1:1,000; Abcam), or anti-F4/80 antibody (1:10; Spring Biosciences) in Antibody

Downloaded from on April 4, 2017

Published August 5, 2013

Diluent, Background Reducing solution (Dako) and visualized using the dual-labeled polymer kit (Envision+; Dako) according to the manufacturer's instructions. Images were captured using the scanner (ScanScope XT; Aperio) and ImageScope software (Aperio).

Cytokine array

The cytokines secreted by Raw 264.7 macrophages were determined using the Proteome Profiler Mouse Cytokine Array kit (R&D Systems) according to the manufacturer's instructions.

In vivo cell labeling and fluorescence imaging

In vivo cell labeling was performed as follows: Vybrant DiI solution (Invitrogen) was used for in vivo labeling of primary mouse pancreatic acinar cells, and Vybrant DiD solution was used for in vivo labeling of Raw 264.7 cells. Labeling was performed according to the manufacturer's instructions. Live cells were photographed in 3D culture medium at 37°C with a fluorescent microscope (IX71; Olympus), a LUCPlan Fluor normal 40×/0.60 NA Ph2 ∞/0–2/FN22 lens, a digital camera (DP70; Olympus), and DP controller software (Olympus) for image acquisition. Images were processed using Photoshop CS3 (Adobe). Immunofluorescence was performed as follows: Sections were subjected to immunofluorescence staining as previously described (Morris et al., 2010a) using rabbit antiamylase (1:200), goat anti–CK-19 (1:100), rat anti-Ly6B.2 (1:3,000), rabbit anti-CD3 (1:200), rat anti-F4/80/EMR1 (1:250), mouse anti-TNF (1:200), and goat anti-RANTES (1:200) as primary antibodies and Alexa Fluor 488, 568/594, or 647 obtained from Invitrogen as secondary antibodies at a 1:500 dilution. DAPI (final concentration of 125 µg/ml) was added when samples were incubated with the secondary antibodies. Fluoromount-G obtained from SouthernBiotech was used as a mounting and imaging medium. Fixed samples were collected at room temperature. Confocal images (Fig. 3, D and E) were collected on a confocal microscope (LSM 510 Meta; Carl Zeiss; LUCPlan Fluor normal 20×/0.45 NA Ph1 ∞/0–2/FN22 and UPlan Flour normal 10×/0.30 NA Ph1 ∞/−/FN26.5 lenses) at consistent gain and offset settings. ZEN software (Carl Zeiss) was used to capture and process confocal images. A ScanScope FL device coupled with ImageScope software was used to capture and process images shown in Fig. 1 (A and D).

RNA isolation and quantitative PCR

Cells were harvested from explant 3D collagen culture by digestion in a 1 mg/ml collagenase solution at 37°C for 30 min on a shaker. Cells were washed once with HBSS and twice with PBS, and total RNA isolation was performed using an RNA isolation kit (miRCURY; Exiqon) and a DNA-free kit (TURBO; Ambion) to eliminate residual genomic DNA. The level of mRNA of interest was assessed using a two-step quantitative reverse transcription–mediated real-time PCR method. Equal amounts of total RNA were converted to cDNA by the high capacity cDNA reverse transcription kit (Applied Biosystems). Quantitative PCR was performed in a real-time thermocycler (7900HT Fast; Applied Biosystems) using the universal PCR master mix (TaqMan; Applied Biosystems) with probe/primer sets and the following thermocycler program: 95°C for 20 s, 40 cycles of 95°C for 1 s, and 60°C for 20 s. All probe/primer sets for mouse acinar and ductal markers or MMPs were purchased from Applied Biosystems (Mm00439508_m1 for MMP-2, Mm00440295_m1 for MMP-3, Mm004487724_m1 for MMP-7, Mm00439509_m1 for MMP-8, Mm00442991_m1 for MMP-9, Mm00444629_m1 for MMP-10, Mm00485048_m1 for MMP-11, Mm00500554_m1 for MMP-12, Mm01168713_m1 for MMP-13, and Mm00491300_m1 for MMP-19). The amplification data were collected by a sequence detector (Prism 7900; Applied Biosystems) and analyzed with Sequence Detection System software (Applied Biosystems). Data were normalized to murine GAPDH, and mRNA abundance was calculated using the $\Delta\Delta C_T$ method. Quantitative real-time PCR with the mouse NF-κB Signaling Targets PCR Array obtained from SABiosciences was performed according to the manufacturer's instructions, and data were analyzed with the web-based RT^2 Profiler PCR Array software (SABiosciences).

Reporter gene assays

Primary mouse pancreatic acinar cells were isolated, infected with adenovirus-NF-κB–luciferase adenovirus (at 10^7 ifu/ml), and immediately plated on a collagen-coated surface and overlayed with Raw 264.7–conditioned or control (Waymouth) media. 24 and 48 h after infection, cells were isolated from collagen, collected, washed with ice-cold PBS, lysed using 250 µl Passive Lysis Buffer (Promega), and centrifuged (13,000 rpm for 10 min at 4°C). Assays for luciferase activity were performed according to the luciferase assay protocol (Promega) and measured using a luminometer (Veritas; Symantec) and GloMax software (Promega). Cell lysates were loaded on a SDS gel, and equal protein expression under different treatment conditions was controlled by silver gel.

Cellular extracts and immunoblotting

Cells were harvested from explant 3D collagen culture by digestion in a 1 mg/ml collagenase solution at 37°C for 30 min on a shaker. Cells were washed once with HBSS and twice with PBS and lysed in buffer A (50 mM Tris/HCl, pH 7.4, 1% Triton X-100, 150 mM NaCl, and 5 mM EDTA) supplemented with protease inhibitor cocktail (Sigma-Aldrich). Lysates were incubated on ice for 30 min and centrifuged (13,000 rpm for 15 min at 4°C), and supernatants were subjected to SDS-PAGE. Gels were either stained by silver gel staining (Silver Stain kit; Thermo Fisher Scientific), or resolved proteins were transferred to nitrocellulose membranes. Membranes were blocked with 5% BSA in TBST (50 mM Tris/HCl, pH 7.4, 150 mM NaCl, and 0.1% Tween 20) and incubated with primary antibodies of interest in 5% BSA in TBST overnight at 4°C and then with horseradish peroxidase–conjugated secondary antibodies for 1 h at room temperature. Samples were visualized with ECL and x-ray film.

Zymography

The supernatant of primary acinar cells in 3D collagen culture was collected and further concentrated using centrifugal filter units with a 30-kD cutoff (EMD Millipore). Samples were mixed with 2× loading buffer (50 mM Tris-HCl, pH 6.8, 10% [vol/vol] glycerol, 1% [wt/vol] SDS, and 0.01% [wt/vol] bromophenol blue) and resolved on an SDS polyacrylamide gel containing 0.12 mg/ml gelatin (porcine skin type A and bloom 300). Gels were soaked in 2.5% Triton X-100 for 1 h, washed twice with collagenase buffer (50 mM Tris-HCl, pH 7.6, 0.2 M NaCl, 5 mM $CaCl_2$, and 0.2% Brij-35), and incubated at 37°C for 18 h. Gels were then washed with distilled water and incubated in Coomassie brilliant blue staining solution (40% methanol and 10% acetic acid/0.025% Coomassie brilliant blue R-250) at room temperature for 2 h. Gels were then washed in distilled water for 2 h and scanned using a scanner (HP Scanjet 4890; Hewlett-Packard).

Human samples

Human formalin-fixed paraffin-embedded pancreatic tissues used in this study were obtained through the Biospecimen Resource for Pancreas Research of the Mayo Clinic SPORE (Specialized Program of Research Excellence) in Pancreatic Cancer. Chronic pancreatitis patients who were undergoing surgical resection and whose diagnoses were clinically and pathologically confirmed provided informed consent as approved by the Institutional Review Board at the Mayo Clinic. Secretin-stimulated exocrine pancreatic secretions were collected in compliance with the Mayo Clinic Institutional Board Review from December 2007 to July 2008 and included normal individuals and patients with pancreatitis.

Statistical analysis

Data are presented as means ± SD. P-values were acquired with the Student's *t* test using Prism (GraphPad Software), and $P < 0.05$ is considered statistically significant.

Online supplemental material

Fig. S1 shows the impact of macrophage depletion on KrasG12D-induced PanIN formation and on the presence of other immune cells in the pancreas. Fig. S2 shows supporting information related to Fig. 2. Fig. S3 shows cytokine identity and position on the cytokine profiler array shown in Fig. 3 A and also detection and quantitation of TNF and RANTES in pancreatic juice. Fig. S4 shows supporting information related to Fig. 4. Fig. S5 shows identification of NF-κB target genes that are expressed in acinar cells when NF-κB1 is virally transduced. Online supplemental material is available at http://www.jcb.org/cgi/content/full/jcb.201301001/DC1.

We thank R. Panayiotou for help with setting up the explant culture method and J. Bachhofer for help with editing the manuscript. We also thank Lizhi Zhang, Ryan Wuertz, and William Bamlet for assistance with identifying patient samples as well as Brandy H. Edenfield of the Mayo Clinic Jacksonville Histopathology Facility for processing and IHC of samples.

This work was supported by a grant from the American Association for Cancer Research (08-20-25-STOR) to P. Storz and the National Institutes of Health grants CA159222 to H.C. Crawford and CA135102 and CA140182 to P. Storz as well as P50CA102701 (Mayo Clinic SPORE in Pancreatic Cancer) to P. Storz. The content is solely the responsibility of the authors and does not necessarily represent the official views of the National Cancer Institute or the National Institutes of Health. The funders had no role in study design, data collection and analysis, decision to publish, or preparation of the manuscript.

Downloaded from on April 4, 2017

Published August 5, 2013

We also thank the Pancreatic Cancer Action Network and the Boshell Foundation for their support.

Author contributions: G.-Y. Liou and H. Döppler performed and analyzed the experiments. G.-Y. Liou, H. Döppler, and P. Storz designed the experiments. P. Storz wrote the manuscript. H.C. Crawford, B. Necela, M. Raimondo, and M. Krishna provided mice, samples, tools, or pathological advice.

Submitted: 1 January 2013
Accepted: 2 July 2013

References

Albazaz, R., C.S. Verbeke, S.H. Rahman, and M.J. McMahon. 2005. Cyclooxygenase-2 expression associated with severity of PanIN lesions: a possible link between chronic pancreatitis and pancreatic cancer. *Pancreatology*. 5:361–369. http://dx.doi.org/10.1159/000086536

Ardito, C.M., B.M. Grüner, K.K. Takeuchi, C. Lubeseder-Martellato, N. Teichmann, P.K. Mazur, K.E. Delgiorno, E.S. Carpenter, C.J. Halbrook, J.C. Hall, et al. 2012. EGF receptor is required for KRAS-induced pancreatic tumorigenesis. *Cancer Cell*. 22:304–317. http://dx.doi.org/10.1016/j.ccr.2012.07.024

Bardeesy, N., and R.A. DePinho. 2002. Pancreatic cancer biology and genetics. *Nat. Rev. Cancer*. 2:897–909. http://dx.doi.org/10.1038/nrc949

Ben-Neriah, Y., and M. Karin. 2011. Inflammation meets cancer, with NF-κB as the matchmaker. *Nat. Immunol.* 12:715–723. http://dx.doi.org/10.1038/ni.2060

Bonal, C., and P.L. Herrera. 2008. Genes controlling pancreas ontogeny. *Int. J. Dev. Biol.* 52:823–835. http://dx.doi.org/10.1387/ijdb.072444cb

Cano, D.A., M. Hebrok, and M. Zenker. 2007. Pancreatic development and disease. *Gastroenterology*. 132:745–762. http://dx.doi.org/10.1053/j.gastro.2006.12.054

Carrière, C., E.S. Seeley, T. Goetze, D.S. Longnecker, and M. Korc. 2007. The Nestin progenitor lineage is the compartment of origin for pancreatic intraepithelial neoplasia. *Proc. Natl. Acad. Sci. USA*. 104:4437–4442. http://dx.doi.org/10.1073/pnas.0701117104

Chandler, N.M., J.J. Canete, and M.P. Callery. 2004. Increased expression of NF-kappa B subunits in human pancreatic cancer cells. *J. Surg. Res.* 118:9–14. http://dx.doi.org/10.1016/S0022-4804(03)00354-8

Chu, G.C., A.C. Kimmelman, A.F. Hezel, and R.A. DePinho. 2007. Stromal biology of pancreatic cancer. *J. Cell. Biochem.* 101:887–907. http://dx.doi.org/10.1002/jcb.21209

Collins, M.A., F. Bednar, Y. Zhang, J.C. Brisset, S. Galbán, C.J. Galbán, S. Rakshit, K.S. Flannagan, N.V. Adsay, and M. Pasca di Magliano. 2012. Oncogenic Kras is required for both the initiation and maintenance of pancreatic cancer in mice. *J. Clin. Invest.* 122:639–653. http://dx.doi.org/10.1172/JCI59227

Coussens, L.M., and Z. Werb. 2002. Inflammation and cancer. *Nature*. 420:860–867. http://dx.doi.org/10.1038/nature01322

Crawford, H.C., C.R. Scoggins, M.K. Washington, L.M. Matrisian, and S.D. Leach. 2002. Matrix metalloproteinase-7 is expressed by pancreatic cancer precursors and regulates acinar-to-ductal metaplasia in exocrine pancreas. *J. Clin. Invest.* 109:1437–1444.

Daniluk, J., Y. Liu, D. Deng, J. Chu, H. Huang, S. Gaiser, Z. Cruz-Monserrate, H. Wang, B. Ji, and C.D. Logsdon. 2012. An NF-κB pathway-mediated positive feedback loop amplifies Ras activity to pathological levels in mice. *J. Clin. Invest.* 122:1519–1528. http://dx.doi.org/10.1172/JCI59743

Esni, F., Y. Miyamoto, S.D. Leach, and B. Ghosh. 2005. Primary explant cultures of adult and embryonic pancreas. *Methods Mol. Med.* 103:259–271.

Fukuda, A., S.C. Wang, J.P. Morris IV, A.E. Folias, A. Liou, G.E. Kim, S. Akira, K.M. Boucher, M.A. Firpo, S.J. Mulvihill, and M. Hebrok. 2011. Stat3 and MMP7 contribute to pancreatic ductal adenocarcinoma initiation and progression. *Cancer Cell*. 19:441–455. http://dx.doi.org/10.1016/j.ccr.2011.03.002

Funahashi, H., M. Satake, D. Dawson, N.A. Huynh, H.A. Reber, O.J. Hines, and G. Eibl. 2007. Delayed progression of pancreatic intraepithelial neoplasia in a conditional Kras(G12D) mouse model by a selective cyclooxygenase-2 inhibitor. *Cancer Res.* 67:7068–7071. http://dx.doi.org/10.1158/0008-5472.CAN-07-0970

Gress, T.M., F. Müller-Pillasch, M.M. Lerch, H. Friess, M. Büchler, and G. Adler. 1995. Expression and in-situ localization of genes coding for extracellular matrix proteins and extracellular matrix degrading proteases in pancreatic cancer. *Int. J. Cancer*. 62:407–413. http://dx.doi.org/10.1002/ijc.2910620409

Guerra, C., A.J. Schuhmacher, M. Cañamero, P.J. Grippo, L. Verdaguer, L. Pérez-Gallego, P. Dubus, E.P. Sandgren, and M. Barbacid. 2007. Chronic pancreatitis is essential for induction of pancreatic ductal adenocarcinoma by K-Ras oncogenes in adult mice. *Cancer Cell*. 11:291–302. http://dx.doi.org/10.1016/j.ccr.2007.01.012

Guerra, C., M. Collado, C. Navas, A.J. Schuhmacher, I. Hernández-Porras, M. Cañamero, M. Rodriguez-Justo, M. Serrano, and M. Barbacid. 2011. Pancreatitis-induced inflammation contributes to pancreatic cancer by inhibiting oncogene-induced senescence. *Cancer Cell*. 19:728–739. http://dx.doi.org/10.1016/j.ccr.2011.05.011

Gukovsky, I., A.S. Gukovskaya, T.A. Blinman, V. Zaninovic, and S.J. Pandol. 1998. Early NF-kappaB activation is associated with hormone-induced pancreatitis. *Am. J. Physiol.* 275:G1402–G1414.

Hingorani, S.R., E.F. Petricoin, A. Maitra, V. Rajapakse, C. King, M.A. Jacobetz, S. Ross, T.P. Conrads, T.D. Veenstra, B.A. Hitt, et al. 2003. Preinvasive and invasive ductal pancreatic cancer and its early detection in the mouse. *Cancer Cell*. 4:437–450. http://dx.doi.org/10.1016/S1535-6108(03)00309-X

Holland, A.M., M.A. Hale, H. Kagami, R.E. Hammer, and R.J. MacDonald. 2002. Experimental control of pancreatic development and maintenance. *Proc. Natl. Acad. Sci. USA*. 99:12236–12241. http://dx.doi.org/10.1073/pnas.192255099

Hruban, R.H., N.V. Adsay, J. Albores-Saavedra, C. Compton, E.S. Garrett, S.N. Goodman, S.E. Kern, D.S. Klimstra, G. Klöppel, D.S. Longnecker, et al. 2001. Pancreatic intraepithelial neoplasia: a new nomenclature and classification system for pancreatic duct lesions. *Am. J. Surg. Pathol.* 25:579–586. http://dx.doi.org/10.1097/00000478-200105000-00003

Lee, F.S., J. Hagler, Z.J. Chen, and T. Maniatis. 1997. Activation of the IkappaB alpha kinase complex by MEKK1, a kinase of the JNK pathway. *Cell*. 88:213–222. http://dx.doi.org/10.1016/S0092-8674(00)81842-5

Lo, B., G. Strasser, M. Sagolla, C.D. Austin, M. Junttila, and I. Mellman. 2012. Lkb1 regulates organogenesis and early oncogenesis along AMPK-dependent and -independent pathways. *J. Cell Biol.* 199:1117–1130. http://dx.doi.org/10.1083/jcb.201208080

Means, A.L., I.M. Meszoely, K. Suzuki, Y. Miyamoto, A.K. Rustgi, R.J. Coffey Jr., C.V. Wright, D.A. Stoffers, and S.D. Leach. 2005. Pancreatic epithelial plasticity mediated by acinar cell transdifferentiation and generation of nestin-positive intermediates. *Development*. 132:3767–3776. http://dx.doi.org/10.1242/dev.01925

Miyatsuka, T., H. Kaneto, T. Shiraiwa, T.A. Matsuoka, K. Yamamoto, K. Kato, Y. Nakamura, S. Akira, K. Takeda, Y. Kajimoto, et al. 2006. Persistent expression of PDX-1 in the pancreas causes acinar-to-ductal metaplasia through Stat3 activation. *Genes Dev.* 20:1435–1440. http://dx.doi.org/10.1101/gad.1412806

Morris, J.P., IV, D.A. Cano, S. Sekine, S.C. Wang, and M. Hebrok. 2010a. Beta-catenin blocks Kras-dependent reprogramming of acini into pancreatic cancer precursor lesions in mice. *J. Clin. Invest.* 120:508–520. http://dx.doi.org/10.1172/JCI40045

Morris, J.P., IV, S.C. Wang, and M. Hebrok. 2010b. KRAS, Hedgehog, Wnt and the twisted developmental biology of pancreatic ductal adenocarcinoma. *Nat. Rev. Cancer*. 10:683–695. http://dx.doi.org/10.1038/nrc2899

Nakamura, T., T. Kuwai, J.S. Kim, D. Fan, S.J. Kim, and I.J. Fidler. 2007. Stromal metalloproteinase-9 is essential to angiogenesis and progressive growth of orthotopic human pancreatic cancer in parabiont nude mice. *Neoplasia*. 9:979–986. http://dx.doi.org/10.1593/neo.07742

Necela, B.M., W. Su, and E.A. Thompson. 2008. Toll-like receptor 4 mediates cross-talk between peroxisome proliferator-activated receptor gamma and nuclear factor-kappaB in macrophages. *Immunology*. 125:344–358. http://dx.doi.org/10.1111/j.1365-2567.2008.02849.x

Pin, C.L., J.M. Rukstalis, C. Johnson, and S.F. Konieczny. 2001. The bHLH transcription factor Mist1 is required to maintain exocrine pancreas cell organization and acinar cell identity. *J. Cell Biol.* 155:519–530. http://dx.doi.org/10.1083/jcb.200105060

Puri, S., and M. Hebrok. 2010. Cellular plasticity within the pancreas—lessons learned from development. *Dev. Cell*. 18:342–356. http://dx.doi.org/10.1016/j.devcel.2010.02.005

Ringel, J., R. Jesnowski, N. Moniaux, J. Lüttges, J. Ringel, A. Choudhury, S.K. Batra, G. Klöppel, and M. Löhr. 2006. Aberrant expression of a disintegrin and metalloproteinase 17/tumor necrosis factor-alpha converting enzyme increases the malignant potential in human pancreatic ductal adenocarcinoma. *Cancer Res.* 66:9045–9053. http://dx.doi.org/10.1158/0008-5472.CAN-05-3287

Sawey, E.T., J.A. Johnson, and H.C. Crawford. 2007. Matrix metalloproteinase 7 controls pancreatic acinar cell transdifferentiation by activating the Notch signaling pathway. *Proc. Natl. Acad. Sci. USA*. 104:19327–19332. http://dx.doi.org/10.1073/pnas.0705953104

Schlosser, W., S. Schlosser, M. Ramadani, F. Gansauge, S. Gansauge, and H.G. Beger. 2002. Cyclooxygenase-2 is overexpressed in chronic pancreatitis. *Pancreas*. 25:26–30. http://dx.doi.org/10.1097/00006676-200207000-00008

Downloaded from on April 4, 2017

Published August 5, 2013

Segara, D., A.V. Biankin, J.G. Kench, C.C. Langusch, A.C. Dawson, D.A. Skalicky, D.C. Gotley, M.J. Coleman, R.L. Sutherland, and S.M. Henshall. 2005. Expression of HOXB2, a retinoic acid signaling target in pancreatic cancer and pancreatic intraepithelial neoplasia. *Clin. Cancer Res.* 11:3587–3596. http://dx.doi.org/10.1158/1078-0432.CCR-04-1813

Song, S.Y., M. Gannon, M.K. Washington, C.R. Scoggins, I.M. Meszoely, J.R. Goldenring, C.R. Marino, E.P. Sandgren, R.J. Coffey Jr., C.V. Wright, and S.D. Leach. 1999. Expansion of Pdx1-expressing pancreatic epithelium and islet neogenesis in transgenic mice overexpressing transforming growth factor alpha. *Gastroenterology*. 117:1416–1426. http://dx.doi.org/10.1016/S0016-5085(99)70292-1

Storz, P., H. Döppler, J.A. Copland, K.J. Simpson, and A. Toker. 2009. FOXO3a promotes tumor cell invasion through the induction of matrix metalloproteinases. *Mol. Cell. Biol.* 29:4906–4917. http://dx.doi.org/10.1128/MCB.00077-09

Strobel, O., Y. Dor, J. Alsina, A. Stirman, G. Lauwers, A. Trainor, C.F. Castillo, A.L. Warshaw, and S.P. Thayer. 2007. In vivo lineage tracing defines the role of acinar-to-ductal transdifferentiation in inflammatory ductal metaplasia. *Gastroenterology*. 133:1999–2009. http://dx.doi.org/10.1053/j.gastro.2007.09.009

Sumazaki, R., N. Shiojiri, S. Isoyama, M. Masu, K. Keino-Masu, M. Osawa, H. Nakauchi, R. Kageyama, and A. Matsui. 2004. Conversion of biliary system to pancreatic tissue in Hes1-deficient mice. *Nat. Genet.* 36:83–87. http://dx.doi.org/10.1038/ng1273

Tucker, O.N., A.J. Dannenberg, E.K. Yang, F. Zhang, L. Teng, J.M. Daly, R.A. Soslow, J.L. Masferrer, B.M. Woerner, A.T. Koki, and T.J. Fahey III. 1999. Cyclooxygenase-2 expression is up-regulated in human pancreatic cancer. *Cancer Res.* 59:987–990.

Wagner, M., H. Lührs, G. Klöppel, G. Adler, and R.M. Schmid. 1998. Malignant transformation of duct-like cells originating from acini in transforming growth factor transgenic mice. *Gastroenterology*. 115:1254–1262. http://dx.doi.org/10.1016/S0016-5085(98)70098-8

Wang, W., J.L. Abbruzzese, D.B. Evans, L. Larry, K.R. Cleary, and P.J. Chiao. 1999. The nuclear factor-kappa B RelA transcription factor is constitutively activated in human pancreatic adenocarcinoma cells. *Clin. Cancer Res.* 5:119–127.

Zhu, L., G. Shi, C.M. Schmidt, R.H. Hruban, and S.F. Konieczny. 2007. Acinar cells contribute to the molecular heterogeneity of pancreatic intraepithelial neoplasia. *Am. J. Pathol.* 171:263–273. http://dx.doi.org/10.2353/ajpath.2007.061176

Downloaded from on April 4, 2017

Liou et al., http://www.jcb.org/cgi/content/full/jcb.201301001/DC1

THE JOURNAL OF CELL BIOLOGY

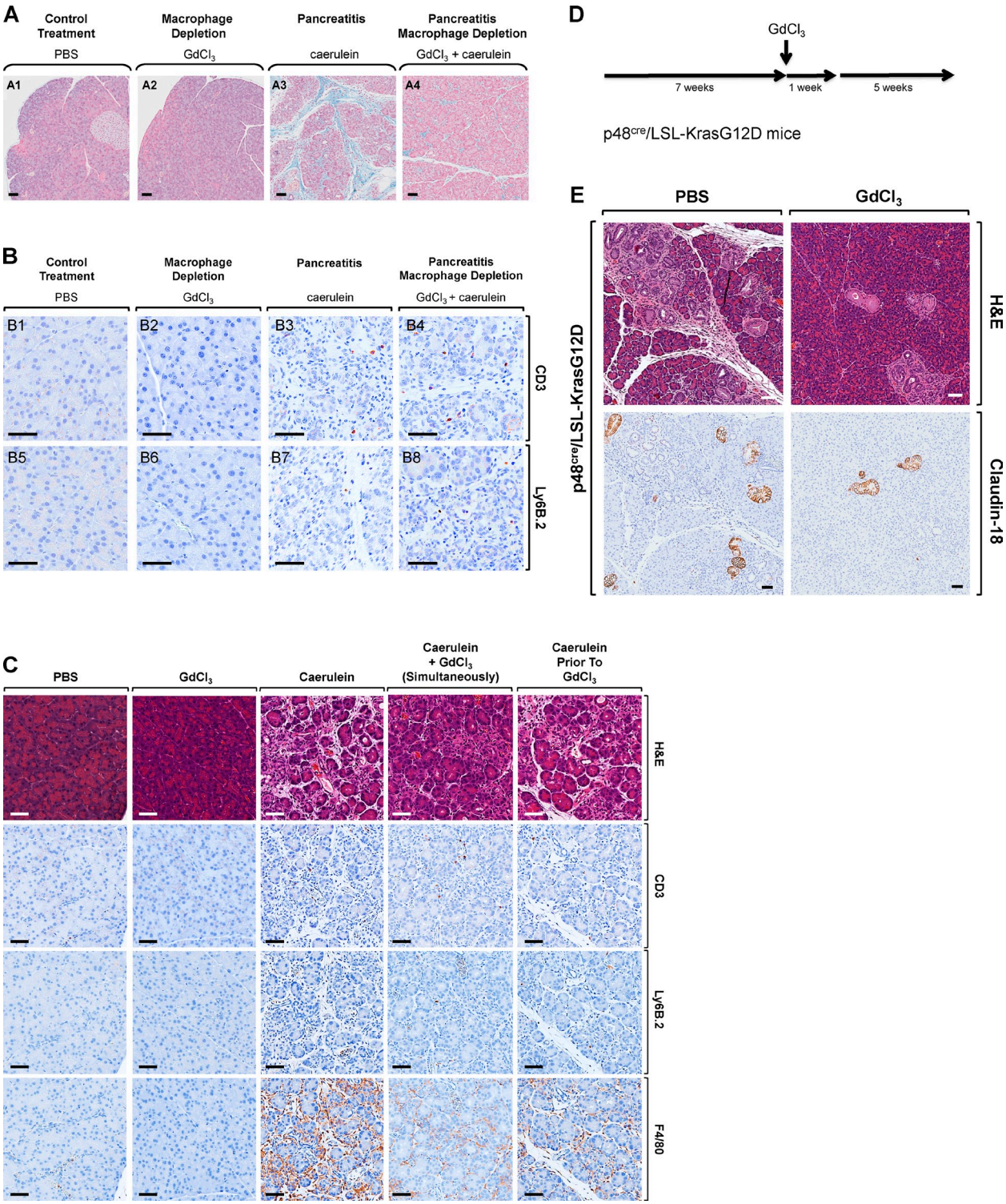

Figure S1. **Impact of macrophage depletion on KrasG12D-induced PanIN formation and on the presence of other immune cells in the pancreas.** (A) FVB mice were treated with control vehicle, $GdCl_3$, caerulein, or a combination, as indicated (detailed method in the Materials and methods section). Pancreata were harvested, and Alcian blue staining was performed. (B) Sections shown in Fig. 1 B were IHC stained for T cells (B1–B4, anti-CD3) and neutrophils (B5–B8, anti-Ly6B.2). Of note, there were no statistical differences between B3 and B4 or B7 and B8 for cell types positive for these markers. (C) At 8 wk of age, mice (n = 3) were intraperitoneally injected with 75 µg/kg caerulein as described in the Materials and methods section. 10 mg/kg $GdCl_3$ was intravenously injected into the tail vein at the same time as the first shot of caerulein (group: caerulein-$GdCl_3$ simultaneously) or immediately after the last shot of caerulein at the second day of caerulein treatment (group: caerulein followed by $GdCl_3$). Pancreata were harvested at day 2 after caerulein treatment and analyzed (H&E and IHC for indicated immune cell markers as described in B). A representative area of the pancreas tissues under each condition is shown. (D and E) At 7 wk of age, $p48^{cre}$/LSL-K-rasG12D mice (n = 3 per condition) were injected as indicated. 10 mg/kg $GdCl_3$ was intravenously injected through the tail vein every 2 d for 1 wk. At the endpoint (week 13), pancreata were harvested and subjected to IHC for H&E and claudin-18. A representative area of the pancreas tissue under each condition is shown. Bars, 50 µm.

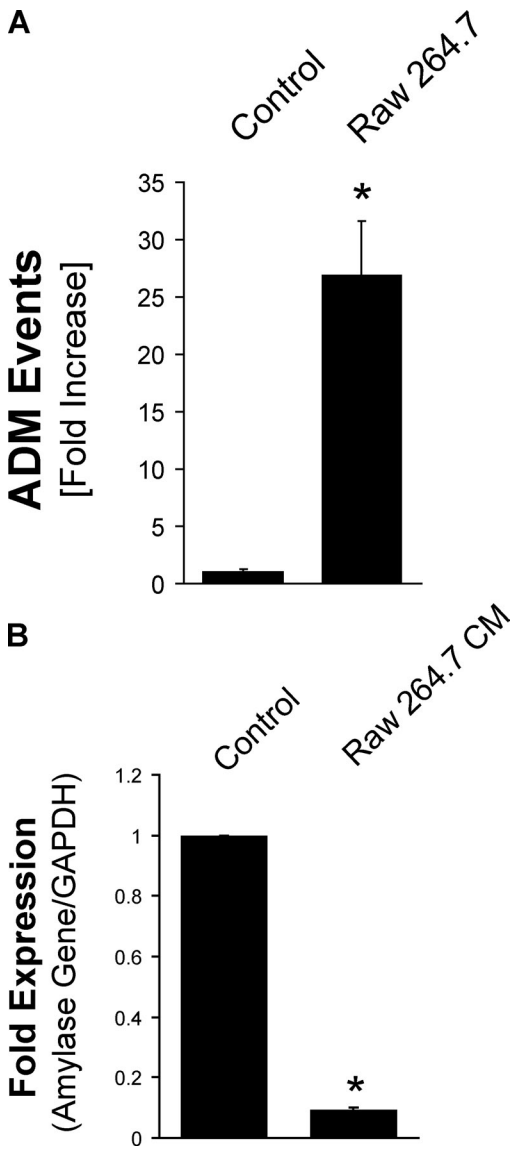

Figure S2. **Supporting information related to Fig. 2.** (A) Quantification of ADM events in co-cultures of Raw 264.7 and pancreatic primary acinar cells. Raw 264.7 and freshly isolated mouse primary acinar cells were co-cultured in 3D collagen explant culture. At day 6, ADM events per well were quantified by counting. (B) Primary mouse pancreatic acinar cells were isolated and treated with Raw 264.7–conditioned media (CM) to induce ADM. At day 8, cells were isolated from the 3D collagen explant culture, and quantitative PCR for amylase expression as a marker for acinar cells was performed and normalized to GAPDH expression. Bar graphs show means ± SD of $n = 3$ experiments (asterisks show statistical significance relative to the control).

A

Coordinate	Target/control	Alternative Nomenclature	Raw 264.7	WR19M.1	Primary
A1, A2	Positive Control	Control (+)			
A23, A24	Positive Control	Control (+)			
B1, B2	BLC	CXCL13/ BCA-1			
B3, B4	C5a	Complement Component 5a			
B5, B6	G-CSF	–			
B7, B8	GM-CSF	–			
B9, B10	I-309	CCL1/TCA-3			
B11, B12	Eotaxin	CCL11			
B13, B14	sICAM-1	CD54			
B15, B16	IFN-γ				
B17, B18	IL-1α	IL-1F1			
B19, B20	IL-1β	IL-1F2			
B21, B22	IL-1ra	IL-1F3			
B23, B24	IL-2	–			
C1, C2	IL-3	–			
C3, C4	IL-4	–			
C5, C6	IL-5	–			
C7, C8	IL-6	–			
C9, C10	IL-7	–			
C11, C12	IL-10	–			
C13, C14	IL-13	–			
C15, C16	IL12 p70	–			
C17, C18	IL-16	–			
C19, C20	IL-17	–			
C21, C22	IL-23	–			
C23, C24	IL-27	–			
D1, D2	IP-10	CXCL10/CRG-2			
D3, D4	I-TAC	CXCL11			
D5, D6	KC	–			
D7, D8	M-CSF	–			
D9, D10	JE	CCL2/MCP-1			
D11, D12	MCP-5	CCL12			
D13, D14	MIG	CXCL9			
D15, D16	MIP-1α	CCL3			
D17, D18	MIP-1β	CCL4			
D19, D20	MIP-2	–			
D21, D22	RANTES	CCL5			
D23, D24	SDF-1	CXCL12			
E1, E2	TARC	CCL17			
E3, E4	TIMP-1	–			
E5, E6	TNFα	TNFSF1A			
E7, E8	TREM-1	–			
F1, F2	Positive Control	Control (+)			
F23, F24	PBS (Negative Control)	Control (–)			

B

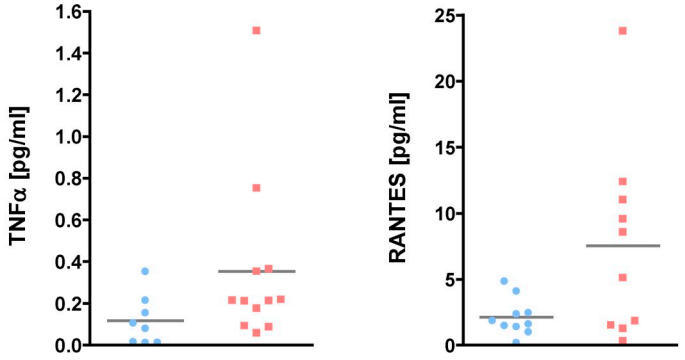

Figure S3. **Cytokine identity and position on the cytokine profiler array shown in Fig. 3 A and detection and quantitation of TNF and RANTES in pancreatic juice.** (A) Table indicating cytokine identity and position on the mouse cytokine profiler array. Yellow labeling indicates cytokines highly abundant in Raw 264.7–conditioned media, red labeling shows cytokines highly abundant in WR19M.1-conditioned media, and green labeling shows cytokines highly abundant in conditioned media from primary mouse macrophages. (B) Detection and quantification of TNF and RANTES in pancreatic juice from control (blue) or pancreatitis (red) patients. (left graph) The concentration of TNF was determined using the human TNF high sensitivity ELISA kit (eBioscience) according to the manufacturer's instructions. $n = 8$ for control patients; $n = 12$ for pancreatitis patients. (right graph) The concentration of RANTES was determined using the human RANTES ELISA kit (R&D Systems) according to the manufacturer's instructions. $n = 10$ for control patients; $n = 10$ for pancreatitis patients. Data shown in both graphs were from a single representative experiment out of four repeats. Data were plotted using the Prism software. Each dot represents one patient sample. Mean values of the TNF or RANTES concentration in each group were depicted as lines.

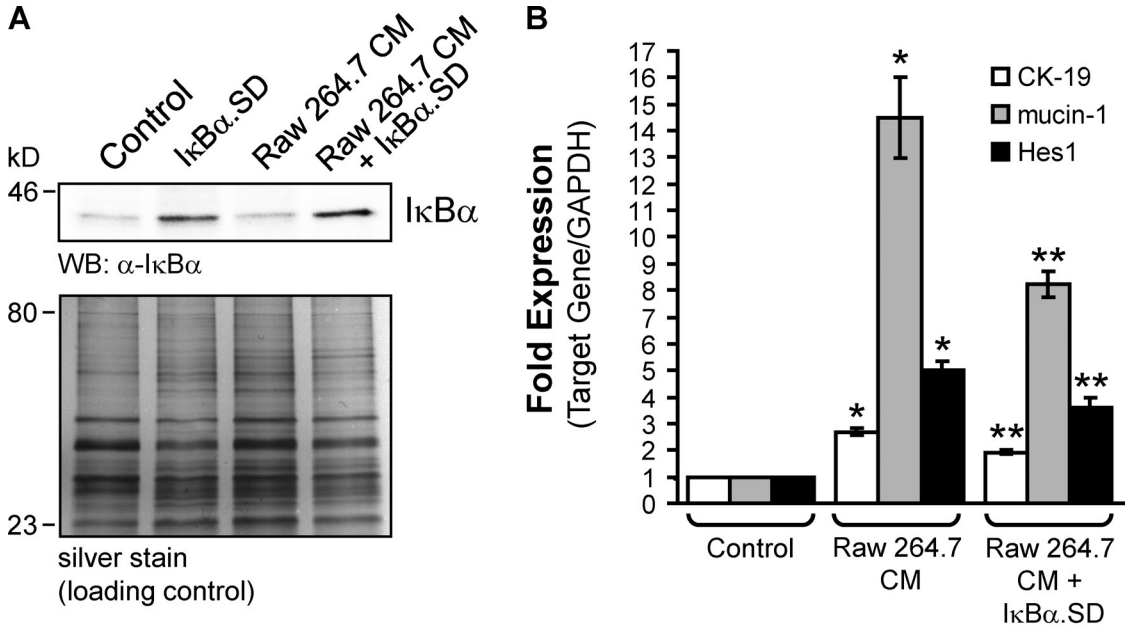

Figure S4. **Supporting information related to Fig. 4.** (A) Primary mouse pancreatic acinar cells were isolated and infected with control virus or adenovirus to express superdominant IκBα (IκBα.SD). At day 6, cells were then cultivated in 3D collagen explant culture in presence of Raw 264.7-conditioned media (CM) or control media as indicated. Cells were harvested from explant 3D collagen culture, lysed and analyzed by Western blotting for IκBα.SD expression using an anti-IκBα antibody. Silver stain of lysates served as a loading control. (B) Primary mouse pancreatic acinar cells were isolated and infected with control virus or adenovirus to express superdominant IκBα (IκBα.SD). Cells were then cultivated in 3D collagen explant culture in the presence of Raw 264.7–conditioned media or control media as indicated. At day 5, cells were harvested from explant 3D collagen culture, and quantitative real-time PCR for ductal markers was performed and normalized to GAPDH expression (single asterisks indicate statistical significance relative to the control; double asterisks indicate statistical significance relative to the stimulus). Bar graphs show means ± SD of *n* = 3 experiments. WB, Western blot.

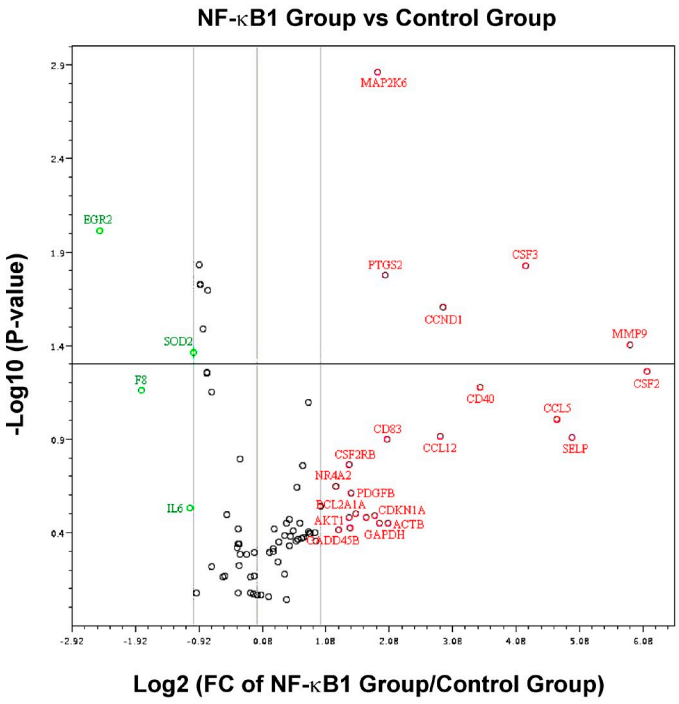

Gene	Fold Change (NF-κB1 VS control)	p value
Adm	1.1921	0.501059
Agt	1.6574	0.420027
Akt1	2.76	0.375142
Aldh3a2	1.4405	0.416482
Bcl2a1a	2.9496	0.316963
Bcl2l1	2.7164	0.330124
Birc2	1.3545	0.662234
Birc3	1.6489	0.174866
C3	-1.2418	0.480302
C4a	-1.8706	0.018807
Ccl12	7.402	0.12206
Ccl22	-1.8706	0.018807
Ccl5	26.5227	0.098369
Ccnd1	7.6343	0.024928
Ccr5	-1.8706	0.018807
Cd40	11.4104	0.066683
Cd74	-1.2204	0.597336
Cd80	-1.3916	0.318993
Cd83	4.1315	0.126587
Cdkn1a	3.6151	0.324014
Cfb	1.1415	0.505576
Csf1	-1.4616	0.688583
Csf2	70.9475	0.054901
Csf2rb	2.7411	0.172619
Csf3	18.758	0.014902
Cxcl1	-1.954	0.839691
Cxcl10	-1.2279	0.38208
Cxcl3	1.3755	0.356165
Cxcl9	-1.8706	0.018807
Egfr	1.4215	0.467588
Egr2	-5.6089	0.009638
F3	1.1318	0.881076
F8	-3.5646	0.069022
Fas	-1.8919	0.014744
Fasl	-1.7243	0.020015
Gadd45b	2.4263	0.384098
Icam1	1.896	0.443567
Ifnb1	-1.8706	0.018807
Ifng	-1.0481	0.852263
Il12b	-1.8706	0.018807
Il15	1.7472	0.080582
Il1a	1.5954	0.356783
Il1b	1.4747	0.387157
Il1r2	1.6304	0.426707
Il1rn	-1.4301	0.677908
Il2	-1.8012	0.03258
Il2ra	-1.7426	0.055184
Il4	-1.8706	0.018807
Il6	-2.0878	0.292969
Ins2	1.3733	0.909442
Irf1	1.2531	0.567917
Lta	-1.7415	0.055725
Ltb	1.5552	0.431023
Map2k6	3.7396	0.001375
Mitf	-1.2321	0.833163
Mmp9	58.6029	0.039539
Myc	-1.1236	0.521081
Myd88	1.191	0.485811
Ncoa3	1.5218	0.444687
Nfkb1	1.4186	0.340311
Nfkb2	1.7582	0.403611
Nfkbia	1.0425	0.853782
Nqo1	-1.0285	0.677482
Nr4a2	2.3537	0.225439
Pdgfb	2.8015	0.245308
Plau	1.7872	0.40526
Ptgs2	4.0435	0.016789
Rel	-1.2212	0.456926
Rela	1.8854	0.396993
Relb	-1.205	0.51855
Sele	1.5409	0.229103
Selp	31.0668	0.123429
Snap25	1.3528	0.414648
Sod2	-2	0.043301
Stat1	1.9917	0.286752
Stat3	1.7428	0.392478
Stat5b	-1.0802	0.837873
Tnf	-1.6463	0.60836
Tnfrsf1b	3.2758	0.332454
Tnfsf10	-1.6519	0.070327
Traf2	-1.2304	0.460337
Trp53	1.2705	0.448031
Vcam1	-1.0303	0.509406
Xiap	-1.079	0.685113

Figure S5. **Identification of NF-κB target genes that are expressed in acinar cells when NF-κB1 is virally transduced.** Primary mouse pancreatic acinar cells from three different mice (biological replicates $n = 3$) were isolated and infected with control virus or adenovirus to express NF-κB1/p105. NF-κB1 target genes in this pathway were determined using quantitative real-time PCR and the mouse NF-κB Signaling Targets PCR Array from SABiosciences as described in Materials and methods. The volcano plot shows fold changes in expression of genes in control acinar cells or cells expressing NF-κB1. The center vertical line indicates no difference between the expression of genes under both conditions. The side vertical lines indicate a twofold difference in either direction. The genes expressed more than twofold in the NF-κB1 group as compared with the control group are labeled in red. The genes expressed lower than twofold in the NF-κB1 group are labeled in green. The horizontal lines (blue) indicate $P < 0.05$. The table shows the fold changes of each gene analyzed. Red labeling indicates up-regulation of twofold or more, and green labeling shows down-regulation of twofold or more. Blue labeling indicates statistical significance $P < 0.05$.